

# Dicopper Alkyl Complexes: Synthesis, Structure, and Unexpected Persistence

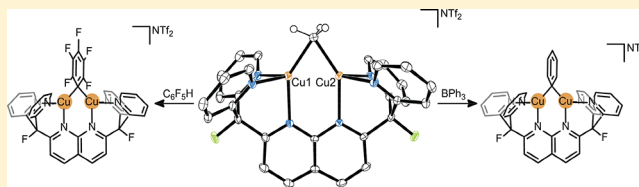
Micah S. Ziegler,<sup>†,‡,§</sup> Nicole A. Torquato,<sup>†</sup> Daniel S. Levine,<sup>†,§</sup> Amélie Nicolay,<sup>†,‡</sup> Hasan Celik,<sup>†</sup> and T. Don Tilley<sup>\*,†,‡,§</sup>

<sup>†</sup>Department of Chemistry, University of California, Berkeley, California 94720-1460, United States

<sup>‡</sup>Chemical Sciences Division, Lawrence Berkeley National Laboratory, Berkeley, California 94720, United States

## Supporting Information

**ABSTRACT:** Cationic  $\mu$ -alkyl dicopper complexes  $[\text{Cu}_2(\mu\text{-}\eta^1\text{-}\eta^1\text{-R})\text{DPFN}]\text{NTf}_2$  ( $\text{R} = \text{CH}_3, \text{CH}_2\text{CH}_3, \text{CH}_2\text{C}(\text{CH}_3)_3$ ; DPFN = 2,7-bis(fluoro-di(2-pyridyl)methyl)-1,8-naphthyridine  $\text{NTf}_2^- = \text{N}(\text{SO}_2\text{CF}_3)_2^-$ ) were synthesized by treatment of the acetonitrile-bridged dicopper complex  $[\text{Cu}_2(\mu\text{-}\eta^1\text{-}\eta^1\text{-NCCH}_3)\text{DPFN}](\text{NTf}_2)_2$  with  $\text{LiR}$  or  $\text{MgR}_2$ . Structural characterization by X-ray crystallography and NMR spectroscopy revealed that the alkyl ligands symmetrically bridge the two copper centers, and the complexes persist in room-temperature solution. Notably, the  $\mu$ -methyl complex showed less than 20% decomposition after 34 days in room-temperature THF solution. Treatment of the  $\mu$ -methyl complex with acids allows installation of a range of monoanionic bridging ligands. However, surprisingly insertion into the dicopper–carbon bond was not observed upon addition of a variety of reagents, suggesting that these complexes exhibit a fundamentally new reactivity profile for alkylcopper species. Electrochemical characterization revealed oxidation–reduction events that evidence putative mixed-valence dicopper alkyl complexes. Computational studies suggest that the dicopper–carbon bonds are highly covalent, possibly explaining their remarkable stability.



## INTRODUCTION

Metal alkyl complexes have long interested chemists, since they provide useful synthetic reagents and catalysts, display unusual bonding motifs, and represent mechanistic intermediates in important transformations.<sup>1–4</sup> Of the many transition-metal alkyl compounds that have been discovered, few have found as wide use in organic and inorganic synthesis as those based on copper.<sup>5</sup> Organocuprates have become especially well known for their selectivity and role in conjugate addition reactions.<sup>6–11</sup> However, in addition to their utility, organocopper compounds have also long been known for their high reactivity and instability.<sup>8,12</sup> Early work by Reich<sup>13</sup> as well as Gilman and Straley<sup>14</sup> highlighted the need for low-temperature preparations that exclude air and water and the lower stability of alkylcopper compounds in comparison to arylcopper analogues.

This elusiveness of isolable alkylcopper compounds is exemplified by methylcopper, which upon warming above 0 °C generally decomposes to give metallic copper, methane, and ethane.<sup>7,15</sup> Use of various ligands, notably phosphines<sup>16</sup> and N-heterocyclic carbenes (NHCs),<sup>17,18</sup> has enabled the isolation and characterization of monomeric alkylcopper complexes that are significantly more persistent under an inert atmosphere. Historically, nitrogen-based ligands have generally not provided similar stabilization.<sup>19–21</sup> Moreover, the bulky or chelating ligands employed to stabilize  $[\text{CuMe}]$  and the propensity for Cu(I) to adopt linear or tetrahedral bonding geometries often result in monocopper structures and therefore neutral complexes.<sup>12</sup> In addition, a range of ionic diorganocuprates, including  $\text{CuMe}_2^-$ , have been isolated and in

the solid state exhibit linear, or nearly linear, binding geometries.<sup>12,22–24</sup>

As described here, the rigid, dinucleating ligand 2,7-bis(fluoro-di(2-pyridyl)methyl)-1,8-naphthyridine (DPFN) that has been shown to support a series of cationic dicopper aryl<sup>25</sup> and alkynyl<sup>26</sup> complexes has provided access to isolable bridging methyl and neopentyl complexes, which have been thoroughly characterized. An ethyl complex was similarly synthesized and, despite slight impurities, studied structurally and spectroscopically. Reactivity accessible to a dicopper–alkyl core was explored by treating the bridging methyl complex with a range of acids and unsaturated compounds. In addition, structural characterization and investigation of the electrochemical properties of the  $\mu$ -methyl complex allow comparisons of alkyl, aryl, and alkynyl ligands bound to a dicopper center. Computational studies corroborate the trends observed in the solid-state structures, and bonded energy decomposition analysis (EDA) suggests a high level of covalency in the interactions between the two copper centers and the bridging carbon atoms.

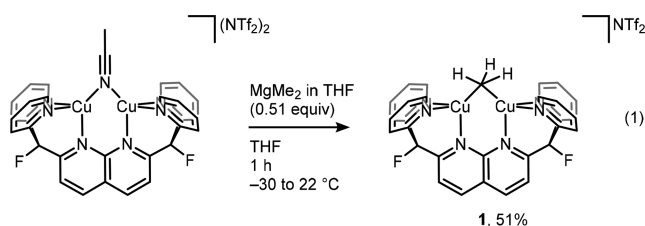
## DICOPPER ALKYL COMPLEXES

Previous work demonstrated that an acetonitrile ligand bridging two copper centers supported by DPFN is displaced by treatment with 1 equiv of tetraphenylborate, from which an aryl group is abstracted to yield a  $\mu$ -Ph ligand.<sup>25</sup> The latter

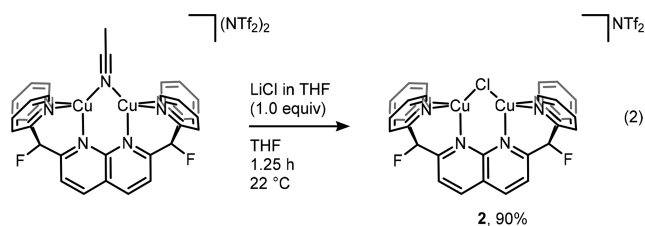
Received: June 28, 2018

complex performs certain C–H bond activations; for example, upon heating for 4 h at 100 °C, the  $\mu$ -Ph complex reacts with a terminal alkyne to generate a  $\mu$ -alkynyl complex and benzene.<sup>26</sup> Significantly harsher conditions were required to activate aryl C–H bonds. For example, exchange of the  $\mu$ -Ph for  $\mu$ -C<sub>6</sub>F<sub>5</sub> upon treatment with excess pentafluorobenzene required heating for 35 days at 110 °C. As alkyl-bridged dicopper complexes were expected to be temperature-sensitive, a lower-temperature approach was sought for the introduction of bridging ligands with sp<sup>3</sup>-hybridized carbon atoms.

Treatment of [Cu<sub>2</sub>( $\mu$ - $\eta^1$ : $\eta^1$ -NCCH<sub>3</sub>)DPFN](NTf<sub>2</sub>)<sub>2</sub> with dimethylmagnesium (0.51 equiv) in THF at –30 °C resulted in a rapid darkening of the reaction mixture. The <sup>1</sup>H NMR spectrum of the primary product revealed a resonance at 0.89 ppm (vs SiMe<sub>4</sub>, in THF-*d*<sub>8</sub>), which integrates to three protons per DPFN ligand. Meanwhile the aromatic resonances suggest that the complex retains its C<sub>2v</sub> symmetry on the NMR time scale. The <sup>19</sup>F NMR spectrum revealed a slight shift of the ligand resonance from –174.50 to –174.32 ppm (vs CFC<sub>3</sub>, in THF), further implying that the dicopper complex undergoes a relatively clean conversion. Together, these spectra indicate that the product is [Cu<sub>2</sub>( $\mu$ - $\eta^1$ : $\eta^1$ -CH<sub>3</sub>)DPFN]NTf<sub>2</sub> (**1**), which was isolated in 51% yield (eq 1).



Other methylating agents were explored for the synthesis of **1**, and methyl lithium (1.1 equiv, 1.6 M in diethyl ether) was also found to afford the bridging methyl complex, in slightly higher yield (63%). However, the resulting product was sometimes contaminated with a small percentage ( $\leq 5\%$ ) of the bridging chloride complex [Cu<sub>2</sub>( $\mu$ -Cl)DPFN]NTf<sub>2</sub> (**2**), which was independently synthesized by treatment of the bridging acetonitrile complex with a solution of LiCl in THF (eq 2).



In the synthesis of **1**, the appearance of **2** very likely results from small amounts of LiCl present in solutions of methyl lithium in diethyl ether.<sup>27,28</sup> Measurably different <sup>1</sup>H and <sup>19</sup>F NMR spectra allow identification and quantification of trace amounts of **2** in solutions of **1**.

Layering diethyl ether over a THF solution of **1** and storage at –35 °C afforded crystals suitable for X-ray diffraction. The solid-state structure of **1** (at 100 K) contains two independent copies of the dicopper cation (one is shown in Figure 1 and Figure S39) in the asymmetric unit and confirms the presence of a bridging methyl group. The methyl ligand bridges nearly symmetrically between the two copper atoms, with all Cu–C distances between 2.060(3) and 2.085(2) Å and all

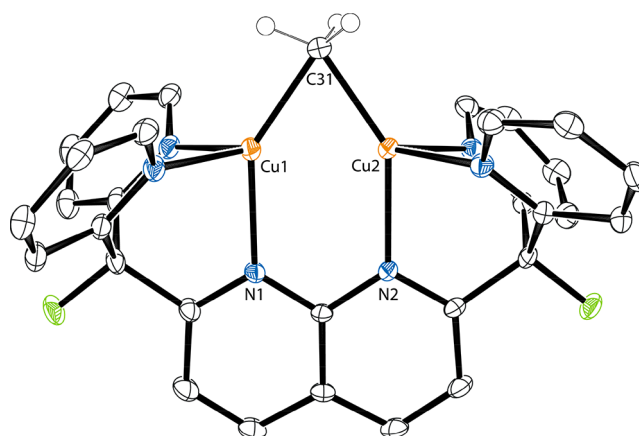


**Figure 1.** Solid-state structure of **1** as determined by single-crystal X-ray diffraction. Only one dicopper cation in the asymmetric unit is shown; the other cation, two NTf<sub>2</sub><sup>–</sup> counterions, and selected hydrogen atoms are omitted for clarity. Thermal ellipsoids are set at the 50% probability level.

$\angle$ C31–Cu<sub>A</sub>–Cu<sub>B</sub> angles between 54.84(8) and 55.84(8)°. The average Cu···Cu distance is 2.3549(3) Å. In addition, the hydrogen atoms on the bridging methyl ligands of both copies of the cation were located in the difference electron density map and refined independently. Their positions imply no significant interactions with the copper atoms.

Recently Molteni and co-workers reported the structure of another methyl-bridged dicopper complex, [Cu(PPh<sub>3</sub>)<sub>2</sub>( $\mu$ -CH<sub>3</sub>)CuCH<sub>3</sub>], which is described as the coordination of a Cu(PPh<sub>3</sub>)<sub>2</sub><sup>+</sup> unit to a nearly linear CuMe<sub>2</sub><sup>–</sup>.<sup>29</sup> In comparison to this donor–acceptor complex, **1** exhibits a shorter Cu···Cu distance (for the donor–acceptor complex Cu···Cu 2.4121(4) Å) and a more symmetrical methyl-binding mode (for the donor–acceptor complex Cu– $\mu$ -CH<sub>3</sub> distances are 2.011(2) and 2.137(2) Å). Ma and co-workers also observed  $\mu$ -CH<sub>3</sub> ligands bridging two metal centers in six-copper clusters.<sup>30</sup> In comparison to **1**, the methyl-bridged units of the clusters also exhibited longer Cu···Cu distances (2.4000(4) and 2.4047(4) Å) and more dissymmetric Cu– $\mu$ -CH<sub>3</sub> distances (averages 1.986(2) and 2.052(2) Å).

Complex **1** joins a series of nearly symmetrically bridged  $\mu$ -methyl complexes of the heavier coinage metals: {[SIPr-Ag]<sub>2</sub>( $\mu$ -Me)}(OTf)<sup>31</sup> (SIPr = 1,3-bis(2,6-diisopropylphenyl)imidazolin-2-ylidene) and [Au<sub>2</sub>( $\mu$ -Me)(PMe<sub>2</sub>Ar<sup>Dipp2</sup>)<sub>2</sub>](NTf<sub>2</sub>)<sup>32</sup> (Ar<sup>Dipp2</sup> = C<sub>6</sub>H<sub>3</sub>-2,6-(C<sub>6</sub>H<sub>3</sub>-2,6-<sup>i</sup>Pr<sub>2</sub>)<sub>2</sub>). The silver and gold dinuclear complexes both have M–C and M···M distances (for both, M–C ca. 2.22 Å, M···M 2.71 Å) significantly longer than are observed in **1**. The structure of **1** is also similar to that of trimethylaluminum, a classic organometallic example of three-center, two-electron bonding, which in comparison to **1** exhibits longer M–C distances (for [AlMe<sub>3</sub>]<sub>2</sub> an average of 2.14(1) Å) and a longer M···M distance (for [AlMe<sub>3</sub>]<sub>2</sub> 2.600(4) Å).<sup>33</sup>

In addition, the structure of **1** can be compared to that of analogous [Cu<sub>2</sub>( $\mu$ - $\eta^1$ : $\eta^1$ -C<sub>X</sub>H<sub>Y</sub>)DPFN]<sup>+</sup> cations that establish a series in which the bridging carbon is sp<sup>3</sup>, sp<sup>2</sup>, or sp hybridized (Figure 2). Across the series, the Cu–C distances shorten and  $\angle$ Cu1–C31–Cu2 angles widen, bringing the central carbon closer to the Cu atoms as the carbon adopts more s character in the orbital presumably directed toward the three-center, two-electron bonding interaction. Meanwhile, the Cu···Cu distance does not show a clear trend with hybridization of the

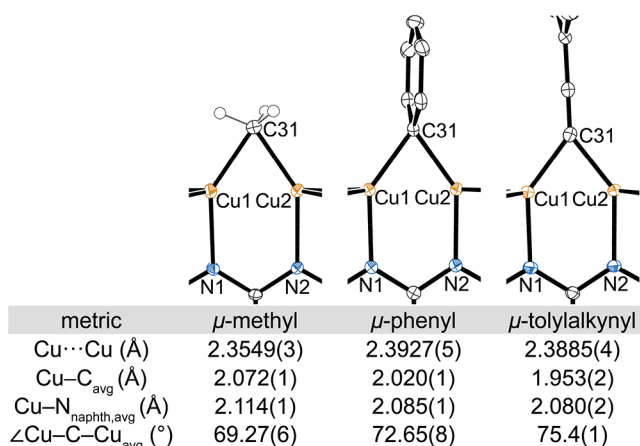


**Figure 2.** Solid-state structures of the dicopper cores of  $[\text{Cu}_2(\mu\text{-}\eta^1\text{:}\eta^1\text{-C}_x\text{H}_y)\text{DPFN}]^+$  cations as determined by single-crystal X-ray diffraction, with key metrics describing the cores' structures. Selected hydrogen atoms are omitted for clarity. Thermal ellipsoids are set at the 50% probability level.

bridging carbon, with the longest distance observed for the  $\mu$ -Ph complex.

The  $^1\text{H}$  and  $^{19}\text{F}$  NMR spectroscopy of **1** in  $\text{THF-}d_8$  revealed that symmetrical binding of the methyl group is maintained in solution on the NMR time scale. The  $\mu\text{-CH}_3$   $^1\text{H}$  resonance at 0.89 ppm (vs  $\text{SiMe}_4$ ) is in a region expected for methyl resonances, while the  $^{13}\text{C}\{^1\text{H}\}$  resonance is found significantly upfield at  $-40.22$  ppm (vs  $\text{SiMe}_4$ ). The carbon resonance was first observed indirectly in a  $^1\text{H}\text{-}^{13}\text{C}$  HSQC experiment (Figure 3b). To confirm that the peak corresponds to a methyl

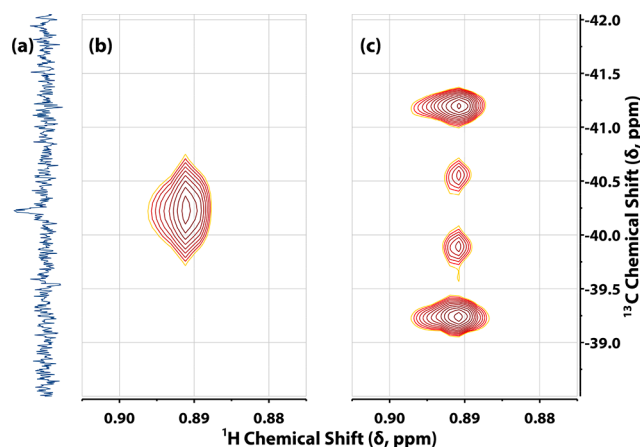


**Figure 3.**  $^{13}\text{C}\{^1\text{H}\}$  (a),  $^1\text{H}\text{-}^{13}\text{C}$  HSQC (b), and proton-coupled  $^1\text{H}\text{-}^{13}\text{C}$  HSQC (c) NMR spectra acquired at 14.1 T (1D experiment) and 16.4 T (2D experiments) of a solution **1** in  $\text{THF-}d_8$ .

moiety, a modified proton-coupled HSQC experiment revealed a 3:1:1:3 quartet pattern characteristic of a methyl group (Figure 3c and Figure S1).<sup>34</sup> This  $^{13}\text{C}$  resonance is upfield of both  $[\text{AlMe}_3]_2$  resonances (bridge  $-5.34$  ppm, terminal  $-8.03$  ppm; at  $-78$  °C in toluene- $d_8$ )<sup>35</sup> as well as the methyl resonances in a range of cuprates,<sup>36</sup>  $\text{CH}_3\text{CuPCy}_3$ ,<sup>37</sup> and the aforementioned dinuclear gold complex ( $-0.1$  ppm).<sup>32</sup> The shift observed for **1** is also upfield of the range of solid-state  $^{13}\text{C}$  chemical shifts reported for Molteni and co-workers' donor-acceptor complex (+1 to  $-16$  ppm)<sup>29</sup> and the solution-state shift reported for Ma and co-workers' hexanuclear cluster ( $-18.99$  ppm).<sup>30</sup>

The one-bond C-H coupling constant ( $^1J_{\text{C-H}}$ ) for the  $\mu\text{-CH}_3$  ligand is 115.8 Hz, below the value expected for an  $\text{sp}^3$ -hybridized carbon atom (i.e., 125 Hz in methane<sup>38</sup>). The coupling constant is similar to those observed in  $[\text{AlMe}_3]_2$  (bridge 112.2 Hz, terminal 115.5 Hz, between  $-60$  and  $-70$  °C)<sup>39</sup> and slightly above those reported for a range of methylcopper complexes generated in situ (108.5–113 Hz).<sup>40</sup> It is also lower than that reported for the  $[\text{Au}_2(\mu\text{-Me})(\text{PMe}_2\text{Ar}^{\text{Dipp}2})_2]^+$  cation (129 Hz).<sup>32</sup>

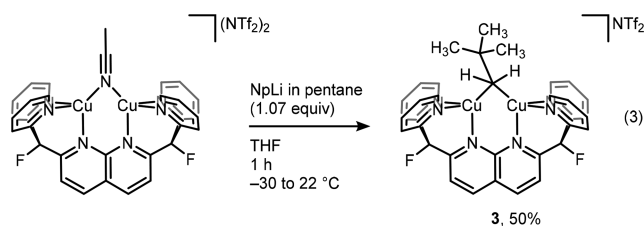
The lack of any methyl resonances in the DPFN ligand and triflimide anion presents an opportunity to observe the vibrational IR modes resulting from the bridging methyl moiety. Upon comparison with the bridging chloride complex, two bands, at 2859 and 2781  $\text{cm}^{-1}$ , in the C-H region were found only in the spectrum of **1** (Figure S2). These bands are tentatively assigned as  $\nu(\text{CH}_3)$  modes. Their relatively low frequencies are consistent with those observed for other bridging  $\text{CH}_3$  groups, especially those of polymeric dimethylmagnesium (2850 and 2780  $\text{cm}^{-1}$ ) and tetrameric methyl-lithium (2840 and 2780  $\text{cm}^{-1}$ ).<sup>41</sup> These frequencies are also similar to some of those reported for  $[\text{Cu}(\text{PPh}_3)_2(\mu\text{-CH}_3)\text{-CuCH}_3]$  (specifically 2852 and 2781  $\text{cm}^{-1}$ ).<sup>29</sup> To bolster the assignment, the IR spectrum of the cation of **1** was calculated employing the  $\omega\text{B97X-D}$  functional<sup>42</sup> and the def2-TZVP basis set. Between 2600 and 3400  $\text{cm}^{-1}$ , three C-H modes were predicted for the bridging methyl moiety, all at energies lower than those for the group of C-H modes for DPFN (Figures S49 and S50). The pattern of the calculated IR frequencies and intensities is consistent with the experimental spectrum of **1** and supports the assignment of the lower energy bands to the bridging methyl ligand.

Surprisingly, **1** is moderately persistent in solution. In room-temperature THF solution, after 1 day approximately 5% decomposition is observed, with 20% observed after 34 days, as determined by  $^1\text{H}$  and  $^{19}\text{F}$  NMR spectroscopy. Upon heating at 60 °C in THF, **1** decomposes over the course of days, accompanied by methane and ethane formation, as observed by  $^1\text{H}$  NMR spectroscopy. Specifically, after 21 days at 60 °C in THF, >93% decomposition of complex **1** was observed, as determined by  $^{19}\text{F}$  NMR (Figure S3). Similar decomposition of **1** was observed in  $\text{THF-}d_8$ ; heating at 60 °C for 23 days afforded >97% decomposition as determined by  $^1\text{H}$  and  $^{19}\text{F}$  NMR spectroscopy (Figures S4 and S5). In the resulting mixture, methane, methane- $d_1$ , and ethane, in a ratio of 1:1.9:1.5, were observed by  $^1\text{H}$  NMR spectroscopy (Figure S6). Formation of methane and ethane is consistent with the products found upon thermal decomposition of phosphine<sup>16,37,43</sup> and NHC-supported<sup>18</sup> methylcopper complexes, except that in the case of **1** no ethylene production was observed.

The persistence of **1** starkly contrasts with that of a range of alkylcopper complexes, notably those supported by nitrogen donor ligands. Solid methylcopper has been reported to persist only at low temperatures and decompose upon warming above approximately 0 °C.<sup>7,15,20,37,44</sup> Previous attempts to stabilize a methylcopper moiety with nitrogen donor ligands, such as 2,2'-bipyridine, similarly led to thermally unstable species.<sup>19,20</sup> A putative anionic dicopper  $\mu$ -methyl complex supported by a tropocoronand macrocycle was also reported to require low-temperature storage.<sup>21</sup> In contrast, coordination of tertiary phosphines to  $[\text{CuMe}]$  moieties imparts greater thermal stability,<sup>16,43,45</sup> as does coordination of N-heterocyclic carbene ligands.<sup>17,18,46</sup> Complex **1** is a rare example of an alkylcopper(I) moiety kinetically stabilized by a nitrogen-based donor ligand. In addition,

**1** is significantly more thermally stable than the aforementioned dicopper  $\mu$ -methyl complex  $[\text{Cu}(\text{PPh}_3)_2(\mu\text{-CH}_3)\text{-CuCH}_3]$ , which is reported to decompose rapidly in solution at room temperature.<sup>29</sup>

Considering the relative stability of the bridging-methyl copper(I) complex in solution, installation of a significantly bulkier alkyl group was attempted. Treatment of  $[\text{Cu}_2(\mu\text{-}\eta^1\text{-}\eta^1\text{-NCCH}_3)\text{DPFN}](\text{NTf}_2)_2$  in THF at  $-30^\circ\text{C}$  with neopentyllithium (1.07 equiv) in pentane provided  $[\text{Cu}_2(\mu\text{-}\eta^1\text{-}\eta^1\text{-CH}_2\text{C}(\text{CH}_3)_3)\text{DPFN}]\text{NTf}_2$  (**3**), which was isolated in 50% yield.



Diffusion of diethyl ether vapor into a THF solution of **3** gave crystals suitable for X-ray diffraction. The solid-state structure contains four copies of the cation in the asymmetric unit (one of which is shown in Figure 4 and Figures S41 and S42)

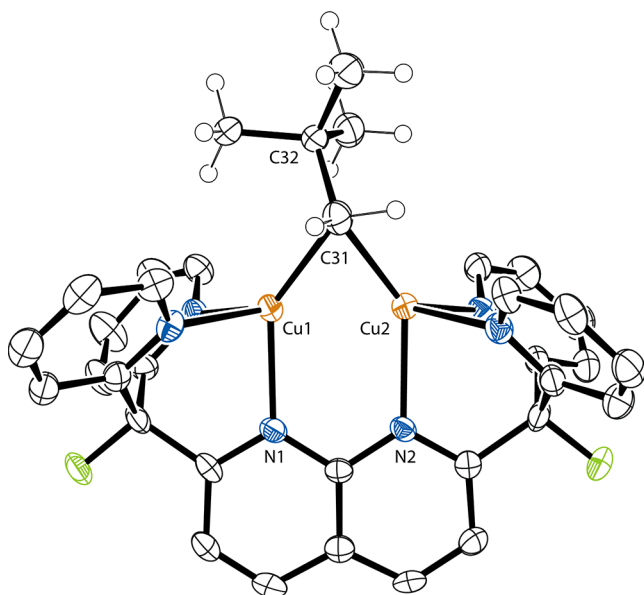


**Figure 4.** Solid-state structure of **3** as determined by single-crystal X-ray diffraction. Only one dicopper cation in the asymmetric unit is shown; the other cations,  $\text{NTf}_2^-$  counterions, four THF molecules of solvation, and selected hydrogen atoms are omitted for clarity. Thermal ellipsoids are set at the 50% probability level.

and reveals that the neopentyl group nearly symmetrically bridges the copper centers, with an average copper–carbon distance of 2.101(2) Å. However, each cation has one shorter Cu–C distance (average 2.084(1) Å) and one longer distance (average 2.119(1) Å), suggesting a slight dissymmetry in the solid state. The average Cu–C distance for the neopentyl complex is longer than that observed for the  $\mu\text{-CH}_3$  complex, as expected considering the added steric bulk, while the average  $\angle\text{Cu1-C31-Cu2}$  angle ( $69.1(1)^\circ$ ) is practically the same as that of the  $\mu\text{-CH}_3$  complex ( $69.27(6)^\circ$ ). The average Cu $\cdots$ Cu distance (2.383(1) Å) is longer than that observed for

the  $\mu\text{-CH}_3$  complex but slightly shorter than those observed for the  $\mu$ -phenyl (2.3927(5) Å) and  $\mu$ -tolylalkynyl (2.3885(4) Å) complexes. The methylene hydrogen atoms for the cation were located in the difference electron density map and refined independently. As with the  $\mu\text{-CH}_3$  complex, the structure does not imply significant interactions between the hydrogen and copper atoms.

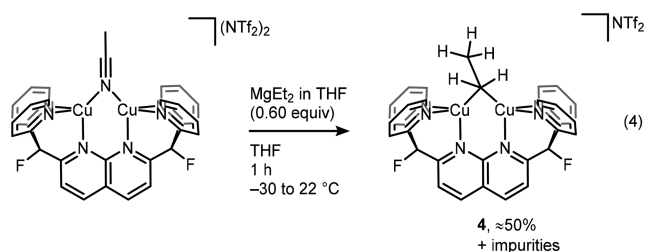
Despite the popularity of neopentyl as a sterically demanding alkyl ligand for transition-metal complexes, few examples of species with bridging neopentyl groups have been reported.<sup>47–52</sup> Notably, a handful of dimanganese complexes have been shown to support bridging neopentyl groups, generally with Mn $\cdots$ Mn distances between 2.685 and 2.718 Å, Mn–C<sub>bridge</sub> distances between 2.185 and 2.645 Å, and  $\angle\text{Mn1-C}_{\text{bridge}}\text{-Mn2}$  angles between  $69.6$  and  $72.7^\circ$ .<sup>47–50</sup> While the metal–metal and metal–carbon distances observed in these dimanganese complexes are significantly longer than those observed in **3**, the metal–carbon–metal angles are quite similar.

While trimethylsilylmethylcopper is a persistent tetramer,<sup>53</sup> an analogous neopentylcopper complex has to our knowledge not been reported. Neopentylcopper species are mentioned as plausible intermediates in reactions between copper halides and Grignard reagents,<sup>54–58</sup> employed as supporting ligands in diorganocuprates for Michael additions,<sup>59</sup> and reported in a phosphine-supported complex,  $\text{Cu}(\text{CH}_2\text{CMe}_3)(\text{PMePh}_2)_3$ .<sup>22</sup> However, these examples do not contain structural characterization of a  $[\text{CuCH}_2\text{CMe}_3]$  unit by X-ray crystallography. In comparison to the bridging trimethylsilylmethyl groups found in the aforementioned tetramer ( $[\text{CuCH}_2\text{Si}(\text{CH}_3)_3]_4$ ), the Cu $\cdots$ Cu distance in **3** is slightly shorter (cf. tetramer 2.418 Å), while the Cu–C distances in **3** are longer (cf. tetramer 2.042 and 1.982 Å). The  $\angle\text{Cu1-C31-Cu2}$  angle in **3** is also more acute (cf. tetramer  $73.84^\circ$ ).

In comparison with the bridging methyl complex, the neopentyl complex is less stable in solution, with approximately 30% decomposing at room temperature over the course of 1 day in THF and 70% over 2 weeks, as determined by  $^1\text{H}$  and  $^{19}\text{F}$  NMR spectroscopy. By  $^1\text{H}$  NMR spectroscopy, the decomposition of **3** in THF- $d_8$  produces a variety of *tert*-butyl-containing products, primarily neopentane, identified by its  $^1\text{H}$  (0.92 ppm vs  $\text{SiMe}_4$ ) and  $^{13}\text{C}$  (31.8 and 27.18 ppm)<sup>60</sup> chemical shifts, which were observed with the aid of  $^1\text{H}$ – $^{13}\text{C}$  HSQC and HMBIC experiments. Of this neopentane, approximately 70% was neopentane- $d_1$  as determined by  $^2\text{H}$  NMR spectroscopy.

A common feature that favors the persistence of metal complexes containing methyl and neopentyl ligands is their lack of  $\beta$ -hydrogen atoms, precluding conversion to a metal hydride via elimination of an alkene.<sup>61,62</sup> To probe the ability of the dicopper–DPFN core to stabilize bridging alkyl groups containing  $\beta$ -hydrogen atoms, installation of a bridging ethyl group was pursued. Similar to the synthesis of **1**, treatment of  $[\text{Cu}_2(\mu\text{-}\eta^1\text{-}\eta^1\text{-NCCH}_3)\text{DPFN}](\text{NTf}_2)_2$  with diethylmagnesium (0.60 equiv) in THF at  $-30^\circ\text{C}$  afforded  $[\text{Cu}_2(\mu\text{-}\eta^1\text{-}\eta^1\text{-CH}_2\text{CH}_3)\text{DPFN}]\text{NTf}_2$  (**4**) in solution (eq 4). While layering diethyl ether over the filtered reaction mixture and storing for 2 days at  $-35^\circ\text{C}$  yielded small crystals of **4**, the product contained a few impurities (Figures S7–S9). Notably,  $^{19}\text{F}$  NMR spectroscopy suggested the presence of more triflimide than expected and small amounts (<2%) of complexes **2** and **6** (vide infra). A range of recrystallization conditions failed to further purify **4**.

Attempts to synthesize the bridging ethyl complex with other reagents also afforded mixtures. Treatment of  $[\text{Cu}_2(\mu\text{-}\eta^1\text{-}\eta^1\text{-NCCH}_3)\text{DPFN}](\text{NTf}_2)_2$  with a commercial ethyllithium solution



(1.1 equiv) yielded a mixture of at least three DPFN-containing products, including approximately 84% of **4** and 12% of **2**, as determined by  $^{19}\text{F}$  NMR spectroscopy. Meanwhile, treatment of the acetonitrile-bridged complex with sodium tetraethylborate (1.0 equiv) gave mixtures primarily composed of **4** and, depending on reaction time, between 20 and 40% of another unidentified DPFN-containing product, as determined by  $^1\text{H}$  and  $^{19}\text{F}$  NMR spectroscopy.

Fortunately, attempts to crystallize **4** from the mixture resulting from reaction with diethylmagnesium afforded crystals suitable for X-ray diffraction. As with complexes **1** and **3**, the solid-state structure of **4** reveals a nearly symmetrically bridging alkyl ligand (Figure 5 and Figures S43 and S44). The

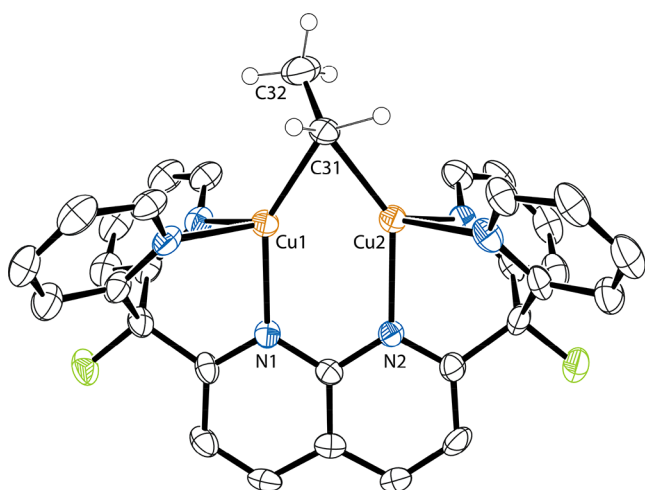


**Figure 5.** Solid-state structure of **4** as determined by single-crystal X-ray diffraction. Disordered  $\text{NTf}_2^-$  counterions, THF molecules of solvation, and selected hydrogen atoms are omitted for clarity. Thermal ellipsoids are set at the 50% probability level.

$\text{Cu}-\text{C}$  distances are 2.082(6) and 2.116(8) Å, suggesting only a slight dissymmetry in the solid state, as was observed for one copy of the bridging methyl complex and all crystallographically independent copies of the bridging neopentyl complex. In addition, the  $\text{Cu}\cdots\text{Cu}$  distance of the bridging ethyl complex (2.362(1) Å) is between those observed for the bridging methyl and neopentyl complexes, while the  $\angle\text{Cu}1-\text{C}31-\text{Cu}2$  angle ( $68.5(2)^\circ$ ) is nearly the same (Table 1). The methylene hydrogen atoms for the  $\mu$ -ethyl ligand were located in the difference electron density map and refined independently. As with the  $\mu$ -methyl and  $\mu$ -neopentyl ligands, significant interactions between the hydrogen and copper atoms were not observed.

$^1\text{H}$  and  $^{19}\text{F}$  NMR spectroscopy of **4** revealed that the bridging ethyl ligand binds symmetrically between the two copper centers on the NMR time scale, as was observed for the bridging methyl and neopentyl ligands. The  $^{13}\text{C}\{^1\text{H}\}$

**Table 1.** Structural and Spectroscopic Data for Dicopper Alkyl DPFN Complexes<sup>a</sup>

metric	$\mu$ -methyl	$\mu$ -ethyl	$\mu$ -neopentyl
$\text{Cu}\cdots\text{Cu}$ (Å)	2.3549(3)	2.362(1)	2.383(1)
$\text{Cu}-\text{C}_{\text{avg}}$ (Å)	2.072(1)	2.099(5)	2.101(2)
$\angle\text{Cu}-\text{C}-\text{Cu}$ (deg)	69.27(6)	68.5(2)	69.1(1)
$\mu$ -C-H chem shift (ppm vs $\text{SiMe}_4$ )	0.89	2.38	1.93
$\mu$ -carbon chem shift (ppm vs $\text{SiMe}_4$ )	-40.22	-21.22	13.02
$\mu$ -C-H $^1J_{\text{C-H}}$ (Hz)	115.8	111.7	107.4
DPFN $^{19}\text{F}$ chem shift (ppm vs $\text{CFCl}_3$ )	-174.31	-173.08	-166.70

<sup>a</sup>NMR spectroscopic data collected in  $\text{THF}-d_8$  at 25 °C.

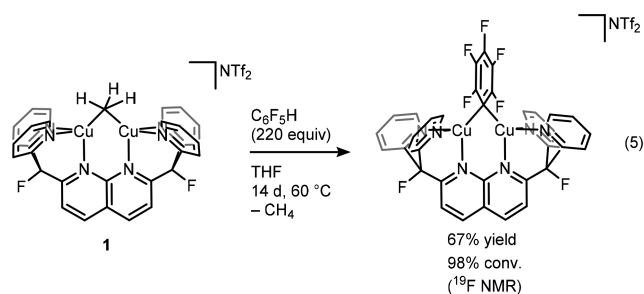
resonance of the bridging methylene was observed directly at -21.22 ppm (vs  $\text{SiMe}_4$ ) and assigned with the aid of a  $^1\text{H}-^{13}\text{C}$  HSQC experiment. The one-bond C-H coupling constant for the bridging ethyl's methylene unit was determined to be 111.7 Hz, while the constant for the ligand's methyl moiety was found to be 123.2 Hz.

Both the  $^{13}\text{C}\{^1\text{H}\}$  chemical shift and C-H coupling constants for the ethyl ligand's bridging carbon are between those observed for the bridging methyl and neopentyl ligands (Table 1). One-bond C-H coupling constants are commonly correlated with their  $\sigma$ -bonds' s character,<sup>38,63-66</sup> and introduction of electropositive substituents onto a carbon atom often lowers the coupling constants of their  $\alpha$ -hydrogens.<sup>67-69</sup> The typical explanation is that electropositive substituents, such as lithium and magnesium, increase electron density on the carbon atom, and the localized hybrid orbital involved in bonding to the metal consumes more s character to better stabilize this density.<sup>67-69</sup> In turn, the carbon atom's remaining hybrid orbitals adopt more p character, weakening their bonds and leading to lower coupling constants. However, in this series of bridging alkyl complexes, the dicopper-DPFN component remains the same while the C-H bond coupling is lowered. Thus, this trend is better explained as the result of increasing steric bulk of the alkyl ligand expanding the dicopper-carbon core, which in turn results in increased electron density at the bridging carbon. The expansion of the  $\text{Cu}_2-\text{C}$  core is indeed observed, as  $\text{Cu}\cdots\text{Cu}$  and  $\text{Cu}-\text{C}_{\text{avg}}$  bond distances increase across the series.

In comparison to complexes **1** and **3**, **4** decomposed rather rapidly in a  $\text{THF}-d_8$  solution at room temperature, reaching 22% decomposition after 17 h, 56% after 41 h, and >98% after 5 days, as determined by  $^1\text{H}$  and  $^{19}\text{F}$  NMR spectroscopy. Monitoring by  $^1\text{H}$  NMR spectroscopy revealed a mixture of many aromatic- and aliphatic-containing decomposition products, including ethane.  $^1\text{H}\{^2\text{H}\}$  NMR spectroscopy indicates that approximately 40% of this ethane was ethane- $d_1$ . However, despite the potential for  $\beta$ -hydrogen elimination, no ethylene formation was observed by  $^1\text{H}$  NMR spectroscopy. Meanwhile,  $^{19}\text{F}$  NMR spectroscopy revealed a range of new fluorine-containing decomposition products, evidenced by the appearance of at least 13 new  $^{19}\text{F}$  resonances, including formation of additional **6** (vide infra). The dicopper ethyl complex's shorter persistence in solution is consistent with early difficulties in the synthesis of ethylcopper<sup>15,19</sup> and later reports suggesting that ethylcopper species generated in situ decompose significantly more quickly than analogous methyl and neopentyl species.<sup>54,56</sup> Similarly, phosphine-<sup>20</sup> and NHC-supported ethylcopper<sup>46</sup> species were found to be considerably less stable than their methylcopper analogues.<sup>17,20</sup>

## REACTIONS OF A DICOPPER METHYL COMPLEX

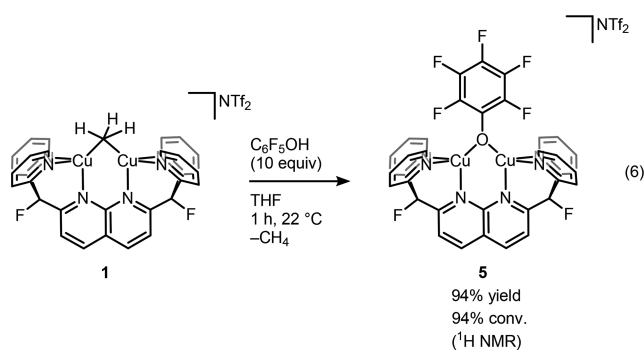
Considering the ability of the  $\mu$ -Ph dicopper complex to activate acidic but strong C–H bonds and exchange the bridging ligand, the reactivity of **1** toward various protic species was investigated. Notably, treatment of **1** with excess pentafluorobenzene and heating at 60 °C afforded  $[\text{Cu}_2(\mu\text{-}\eta^1\text{:}\eta^1\text{-C}_6\text{F}_5)\text{DPFN}]\text{NTf}_2$  in 67% yield (98% conversion) as determined by  $^{19}\text{F}$  NMR spectroscopy (Figure S10), with concomitant generation of methane as determined by  $^1\text{H}$  NMR spectroscopy (eq 5).



The difference between the  $^{19}\text{F}$  NMR determined yield of the  $\mu\text{-C}_6\text{F}_5$  complex and conversion of **1** likely results from ligand exchange of  $-\text{CH}_3$  for  $-\text{C}_6\text{F}_5$  competing with decomposition pathways. In comparison, the same transformation can be accomplished in higher yield, 85% (99% conversion), by heating  $[\text{Cu}_2(\mu\text{-}\eta^1\text{:}\eta^1\text{-Ph})\text{DPFN}]\text{NTf}_2$  with excess pentafluorobenzene in *o*- $\text{C}_6\text{H}_4\text{F}_2$  at 110 °C for 35 days.<sup>25</sup>

Considering its ability to activate strong C–H bonds, **1** was also treated with water, with the goal of generating a bridging hydroxide complex. Unfortunately and unexpectedly, addition of water (ca. 170 equiv) to **1** in THF at room temperature does not cleanly generate a new complex. Rather, in the presence of water, **1** very slowly decomposes at room temperature to a variety of species and after 14 days reaches 96% conversion (as determined by  $^{19}\text{F}$  NMR spectroscopy; Figure S11).

To explore whether a more acidic oxygen-based acid would cleanly react with **1**, a solution of **1** in THF was treated with pentafluorophenol (10 equiv), which nearly quantitatively yielded the bridging phenoxide complex  $[\text{Cu}_2(\mu\text{-}\eta^1\text{:}\eta^1\text{-OC}_6\text{F}_5)\text{DPFN}]\text{NTf}_2$  (**5**) and methane over the course of 1 h at 22 °C, as determined by  $^1\text{H}$  and  $^{19}\text{F}$  NMR spectroscopy (eq 6 and Figures S12 and S13). The same product was obtained upon treatment of the bridging phenyl complex in *o*- $\text{C}_6\text{H}_4\text{F}_2$  with pentafluorophenol, allowing the isolation of **5** in 85% yield.



Vapor diffusion of pentane into a *o*- $\text{C}_6\text{H}_4\text{F}_2$  solution of **5** for 15 days at  $-35$  °C afforded crystals suitable for X-ray diffraction. In comparison to the structures of the bridging  $\text{Cu}_2(\text{I,I})$  alkyl, aryl, and alkynyl complexes, the solid-state structure of **5** (Figure 6 and Figures S45 and S46) reveals a

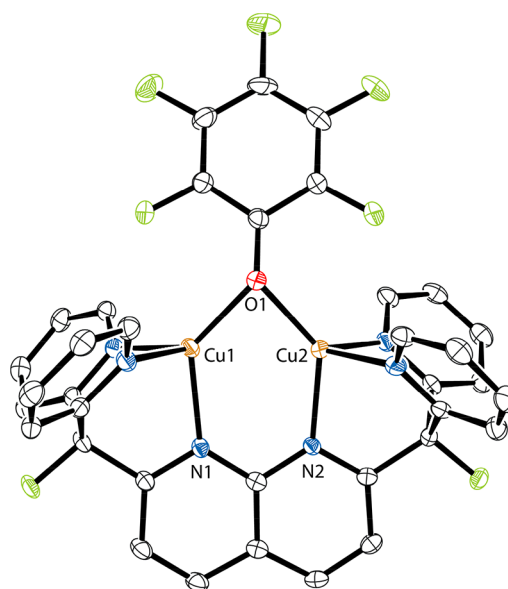
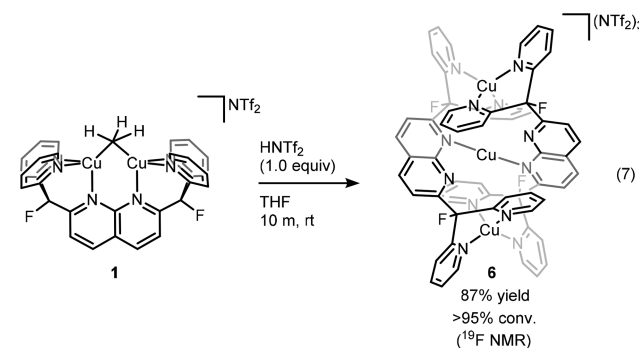


**Figure 6.** Solid-state structure of **5** as determined by single-crystal X-ray diffraction. The  $\text{NTf}_2^-$  counterion, two *o*- $\text{C}_6\text{H}_4\text{F}_2$  molecules, half of a pentane molecule of solvation, and hydrogen atoms are omitted for clarity. Thermal ellipsoids are set at the 50% probability level.

bridging ligand that binds with a much less acute central angle. The Cu–O distances (2.002(2) and 1.989(3) Å) are shorter than the Cu–C distances observed in the bridging methyl and phenyl complexes, and the Cu···Cu distance is significantly longer (2.675(1) Å). As a result, the  $\angle\text{Cu1-O1-Cu2}$  angle ( $84.18(9)^\circ$ ) is wider than that found in the hydrocarbyl series, and the average Cu– $\text{N}_{\text{naphth}}$  distance is shorter.

Within 10 min of treatment with 1 equiv of an even stronger acid,  $\text{HNTf}_2$ , complex **1** in THF forms a tricationic helical complex incorporating three copper centers and two molecules of DPFN (eq 7 and Figure S14). This helix,  $[\text{Cu}_3(\text{DPFN})_2]_-(\text{NTf}_2)_3$  (**6**), was also generated by treatment of the bridging phenyl complex with  $\text{HNTf}_2$  (1.0 equiv) in *o*- $\text{C}_6\text{H}_4\text{F}_2$ , allowing the product to be isolated in 58% yield. Ostensibly, the loss of the dicopper core structure results from the inability of the triflimide anion to provide a viable bridge between two copper centers ligated by DPFN.



Vapor diffusion of hexanes into an *o*- $\text{C}_6\text{H}_4\text{F}_2$  solution of **6** and storage for 4 days at  $-35$  °C afforded crystals suitable for X-ray diffraction, allowing its structure to be elucidated (Figure 7 and Figures S47 and S48). In the solid state, the side-arm pyridine pairs provide pseudotetrahedral ligand environments for two copper centers while the third copper is bound nearly linearly between two naphthyridine nitrogen atoms

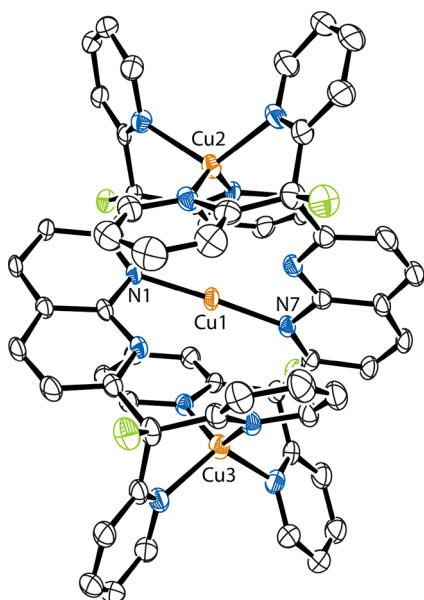
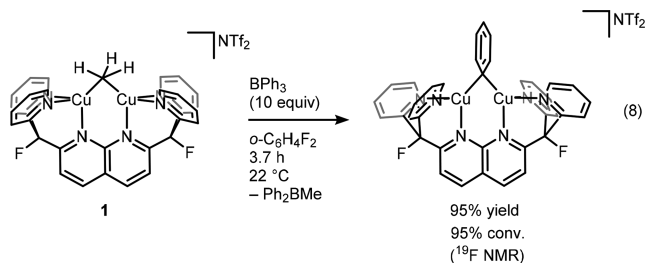


**Figure 7.** Solid-state structure of **6** as determined by single-crystal X-ray diffraction. The  $\text{NTf}_2^-$  counterions, two  $o\text{-C}_6\text{H}_4\text{F}_2$  molecules of solvation, and hydrogen atoms are omitted for clarity. Thermal ellipsoids are set at the 50% probability level.

( $\angle\text{N1-Cu1-N7}$   $174.7(1)^\circ$ ). In addition, the  $\angle\text{Cu2-Cu1-Cu3}$  angle is  $155.66(2)^\circ$ . In  $^1\text{H}$  NMR spectra at room temperature, only one doublet is observed for the 4-position hydrogen on the naphthyridine subunits; in  $^{19}\text{F}$  NMR spectra, a singlet (at  $-148.47$  ppm vs  $\text{CFCl}_3$  in nitrobenzene- $d_5$ ) is observed for the trication. These data suggest that, on the NMR time scale, the central Cu atom interacts similarly with all four central naphthyridine nitrogen atoms.

The reactivity of **1** toward a Lewis acid ( $\text{BPh}_3$ ) was also investigated. Transmetalation from boron to copper, albeit a single copper center in its +2 oxidation state, is predicted to be a key step in the mechanism of various oxidative cross-coupling reactions (e.g., the Chan–Evans–Lam amination).<sup>70–74</sup> Treatment of a  $o\text{-C}_6\text{H}_4\text{F}_2$  solution of **1** with triphenylborane (10 equiv) produced the bridging phenyl complex in nearly quantitative yield (eq 8 and Figures S15 and S16). A new  $^{11}\text{B}$  resonance observed at  $\sim 6$  ppm downfield of that for  $\text{BPh}_3$  suggests that the transformation occurs with the formation of  $\text{BMePh}_2$  (Figure S17).<sup>75,76</sup>



This carbon–boron bond exchange is consistent with the reactivity observed upon treatment of the acetonitrile-bridged complex  $[\text{Cu}_2(\mu\text{-}\eta^1\text{:}\eta^1\text{-NCCCH}_3\text{)DPFN}](\text{NTf}_2)_2$  with tetraarylborato anions, which results in the formation of bridging aryl complexes and triarylboranes.<sup>25</sup> The reaction is also similar to the arylation of a  $\text{Cu}^{\text{II}}\text{O}^t\text{Bu}$   $\beta$ -diketiminato complex, where treatment with  $\text{B}(\text{C}_6\text{F}_5)_3$  resulted in aryl transfer to the copper center, forming a  $\text{Cu}^{\text{II}}\text{C}_6\text{F}_5$  complex.<sup>77</sup>

Organocopper reagents are well-known for their role in conjugate addition to compounds containing  $\alpha,\beta$ -unsaturated carbonyl groups, often in reactions that proceed at low temperatures.<sup>7–10</sup> To explore this reactivity, complex **1** was treated with cyclohexenone (2.1 equiv) in THF. After 6 days at room temperature, no significant consumption of cyclohexenone was observed by  $^1\text{H}$  NMR spectroscopy while **1** appeared to decompose, as determined by  $^1\text{H}$  and  $^{19}\text{F}$  NMR spectroscopy (Figure S18), which showed loss of **1** and methane formation. Heating the mixture to  $80^\circ\text{C}$  for 21 h led to additional decomposition of **1**.

Previously reported methylcopper complexes, supported by phosphine<sup>20,78–80</sup> and NHC<sup>17</sup> ligands, have been shown to react with carbon dioxide to afford copper acetate complexes. Considering this precedence and the ability of **1** to behave as a nucleophile upon treatment with acids, reactivity with carbon dioxide was explored. However, when a solution of **1** in THF- $d_8$  was placed under an atmosphere of carbon dioxide, no significant reaction was observed over the course of 29 h at room temperature, as determined by  $^1\text{H}$  NMR spectroscopy. Heating the mixture at  $60^\circ\text{C}$  for 2 days appeared to lead to slight decomposition of **1**, as suggested by the formation of both methane and methane- $d_1$ .

To determine whether the dicopper methyl complex would insert a sterically unencumbered olefin, a solution of **1** in THF was treated with 1-hexene (ca. 400 equiv). After 1 day at room temperature no significant reactions of complex **1** or the 1-hexene were observed by  $^1\text{H}$  NMR spectroscopy. Subsequent heating of the mixture to  $60^\circ\text{C}$  for 6 days appeared to result in decomposition of the dicopper complex, indicated by the formation of methane and a variety of fluorine-containing products, as determined by  $^1\text{H}$  and  $^{19}\text{F}$  NMR spectroscopy, respectively. Similar results were obtained upon treatment of **1** with diphenylacetylene (13 equiv). When the mixture was heated to  $60^\circ\text{C}$  for 6 days, methane formation and multiple fluorine-containing products appeared, while no consumption of diphenylacetylene was observed, as determined by  $^1\text{H}$  and  $^{19}\text{F}$  NMR spectroscopy.

Taken together, these results suggest that the cationic dicopper–methyl core in **1** possesses weak nucleophilic character and in this way seems quite different from organocuprate reagents. The methyl complex **1** appears to favor reactions with  $\sigma$ -bonds (including C–H, B–C, and O–H bonds, as described above), and delocalization of electron density in the  $\text{Cu}_2\text{–C}$  core appears to mitigate against direct insertion reactions. Thus, **1** represents a fundamentally new type of molecular alkyl-copper complex expected to display distinct reactivity trends and reaction pathways that are yet to be uncovered.

## ■ ELECTROCHEMISTRY OF DICOPPER ALKYL COMPLEXES

Recent discoveries of mixed-valence copper aryl,<sup>25</sup> alkynyl,<sup>26</sup> and hydride<sup>81,82</sup> complexes inspired electrochemical investigation of the dicopper alkyl complexes **1** and **3**. Specifically, dicopper DPFN complexes with bridging aryl<sup>25</sup> and alkynyl<sup>26</sup> ligands were oxidized chemically to afford mixed-valence organocopper species. These dicationic mixed-valence complexes were persistent, allowing for their isolation and the structural and spectroscopic characterization of their  $\text{Cu}_2(\text{I,II})$ –phenyl and  $\text{Cu}_2(\text{I,II})$ –*p*-tolylalkynyl cores. Thus, we sought to determine whether the bridging alkyl complexes would exhibit similar electrochemistry.

Cyclic voltammetry of **1** revealed a reversible oxidation–reduction process at  $E^{o'} = -0.148$  V vs  $[\text{Cp}_2\text{Fe}]^{0/+}$  ( $i_{\text{pa}}/i_{\text{pc}} = 1.01$ ,  $\Delta E_{\text{p}} = 81$  mV, both measured at 100 mV/s, Figure 8a and

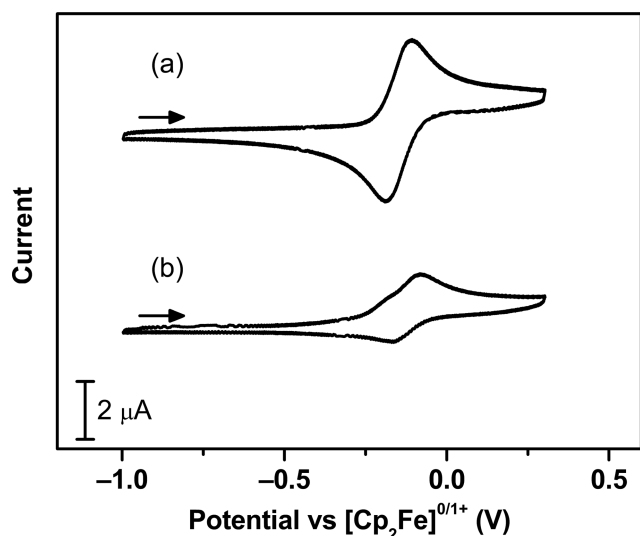


**Figure 8.** Cyclic voltammograms of 0.5 mM solutions of (a) **1** and (b) **3** in *o*-C<sub>6</sub>H<sub>4</sub>F<sub>2</sub> with 0.1 M [<sup>t</sup>Bu<sub>4</sub>N][PF<sub>6</sub>] supporting electrolyte. The arrows indicate the initial potentials and scanning directions. Scan rate: 100 mV/s.

Figures S19–S22). However, voltammetry of **3** revealed a quasireversible wave at a slightly less negative potential ( $E^{o'} = -0.113$  V vs  $[\text{Cp}_2\text{Fe}]^{0/+}$ , measured at 2000 mV/s, Figures S23–S26). At fast scan rates, at and above 1250 mV/s, the event's formal potential remains at  $-0.113$  V and the  $i_{\text{pa}}/i_{\text{pc}}$  ratio is approximately 1.5. At slower scan rates, the  $i_{\text{pa}}/i_{\text{pc}}$  ratio increases, and the reduction wave becomes significantly distorted (Figure 8b and Figures S24 and S25). These results suggest that a putative mixed-valence dicopper neopentyl complex does not significantly persist in room-temperature solution. Similarly, attempts to synthesize and isolate a mixed-valence dicopper methyl complex via chemical oxidation have led to decomposition, suggesting that it too might not persist over longer time scales. The transience of these dicopper alkyl complexes upon oxidation is consistent with previous reports of monomeric NHC-supported copper(I) alkyl complexes decomposing after treatment with one-electron chemical oxidants.<sup>83</sup>

The bridging alkyl groups lead to the most easily oxidized species in the series of dicopper DPFN complexes (Table 2), consistent with alkyl substituents generally donating more electron density than aryl or alkynyl groups. This trend could also be rationalized by the stabilization ability of the electronically delocalized bridging phenyl and tolylalkynyl ligands in comparison to the methyl and neopentyl ligands. Meanwhile, the more electronegative heteroatom-based bridging groups (e.g., OC<sub>6</sub>F<sub>5</sub>, Cl), even though they could conceivably donate density from electrons localized on the heteroatom (i.e., lone pairs), have relatively moderate oxidation potentials (Table 2 and Figures S27–S34) in comparison to the range of those observed for the organic bridging groups with various electron-withdrawing substituents.

## COMPUTATIONAL INSIGHTS

To corroborate our structural observations and investigate the bonding characteristics that might contribute to the unexpected

**Table 2.** Electrochemical Metrics for Reversible and Quasireversible Redox Processes for Dicopper DPFN Complexes<sup>a</sup>

bridging ligand	formal potential (V vs Fc <sup>0/+</sup> )	ratio of peak currents ( $i_{\text{pa}}/i_{\text{pc}}$ )	ref
$\mu$ -CH <sub>3</sub>	-0.148	1.01	this work
$\mu$ -CH <sub>2</sub> C(CH <sub>3</sub> ) <sub>3</sub>	-0.113 <sup>b</sup>	2.03	this work
$\mu$ -C <sub>6</sub> H <sub>5</sub>	-0.014	1.02	25
$\mu$ -(3,5-(CF <sub>3</sub> ) <sub>2</sub> -C <sub>6</sub> H <sub>3</sub> )	0.347	1.12	25
$\mu$ -C <sub>6</sub> F <sub>5</sub>	0.516	1.18	25
$\mu$ -(1,4-bis(4-tolyl)-1,2,3-triazolide)	0.302	1.17	26
$\mu$ -C≡C(C <sub>6</sub> H <sub>4</sub> )CH <sub>3</sub>	0.022	1.04	26
$\mu$ -C≡C(C <sub>6</sub> H <sub>4</sub> )CF <sub>3</sub>	0.120	1.02	this work
$\mu$ -OC <sub>6</sub> F <sub>5</sub>	0.101	1.40	this work
$\mu$ -Cl	0.181	1.15	this work

<sup>a</sup>Metrics measured for 0.5 mM solutions of a given complex in *o*-C<sub>6</sub>H<sub>4</sub>F<sub>2</sub> containing 0.1 M [<sup>t</sup>Bu<sub>4</sub>N][PF<sub>6</sub>] as a supporting electrolyte with a scan rate of 100 mV/s. <sup>b</sup>Estimated from voltammograms obtained at 2000 mV/s.

persistence of the dicopper alkyl complexes, we turned to computations. Gas-phase geometry optimization of the bridging methyl, phenyl, and *p*-tolylalkynyl (truncated in the computations to phenylalkynyl) complexes using the  $\omega$ B97X-D functional<sup>42</sup> and the def2-SVP basis set provided dicopper core geometries (Table 3) generally consistent with those observed

**Table 3.** Calculated Geometry Metrics for Dicopper Hydrocarbyl DPFN Cations

metric	$\mu$ -methyl	$\mu$ -phenyl	$\mu$ -phenylalkynyl
Cu...Cu (Å)	2.35	2.39	2.40
Cu–C <sub>avg</sub> (Å)	2.08	2.03	1.96
$\angle$ Cu–C–Cu (deg)	68.7	72.2	75.7

in the solid-state structures (Figure 2). Notably, in the computed structures, the  $\angle$ Cu–C<sub>bridging</sub>–Cu angles were also found to widen progressing from the methyl complex to the alkynyl, while the average copper–carbon distances shortened. In addition, the Cu...Cu distance is shortest in the methyl complex and longer in the phenyl and alkynyl complexes. These computational results suggest that the trends observed in the solid state are not artifacts of crystal packing.

Investigation of the canonical orbitals calculated for the energy-minimized structure of **1** revealed a bonding orbital that nearly symmetrically bridges the two copper centers and bridging carbon (Figure 9). Analogous orbitals were also found for the  $\mu$ -phenyl and  $\mu$ -phenylalkynyl complexes (Figures S51 and S52). These orbitals are consistent with the expectation of a three-center, two-electron bond supporting the bridging hydrocarbyl ligand.<sup>62,84,85</sup>

The nature of bonding between various bridging ligands and the dicopper core was also investigated by bonded energy decomposition analysis (EDA).<sup>86,87</sup> This method separates the quantum mechanical interaction energy between two molecular fragments into components that correspond to traditional contributors to bonding interactions (e.g., electrostatics, polarization, charge transfer). For a given bonding interaction, this method obtains a chemical “fingerprint” that characterizes the type of bond present. To develop this fingerprint, bonded EDA separates the interaction energy into five components. The first two components are (1) preparation energy, which

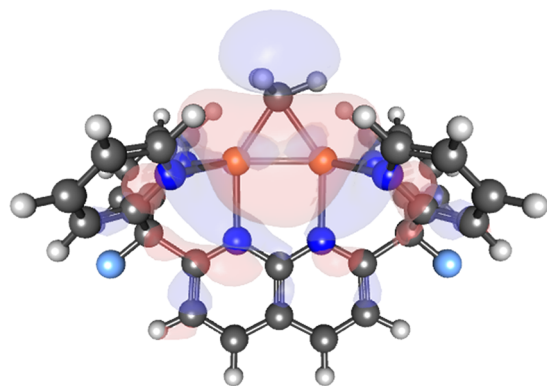


Figure 9. Primarily three-center, two-electron canonical orbital of 1.

corresponds to geometrically and electronically distorting the fragments from their separated states to the states they assume upon interaction, and (2) frozen energy, which is the sum of the individual components' electrostatic, Pauli repulsion, and dispersion energies. These first two components are nearly always positive because they represent the geometric/electronic destabilization of the fragments and the Pauli repulsion/electrostatics upon their interaction, respectively. The next three components are generally stabilizing and include (3) spin-coupling energy, which estimates covalency by determining how much energy is gained by coupling the bonding electrons, (4) polarization energy, which relates how electrons on each fragment respond to the electric field of the other fragment, and (5) charge-transfer energy, which measures the energy gained from electrons fluctuating into ionic-like states between the two fragments—a process that occurs even in symmetric bonds.

The EDA results for complexes 1 and 5, as well as for the bridging phenyl and alkynyl complexes for comparison, are displayed in Table 4. Progressing from methyl ( $sp^3$ ) to aryl ( $sp^2$ ) to alkynyl ( $sp$ ), the more stabilizing (more negative) spin-coupling component is consistent with the covalent character of the  $Cu_2-C$  bonding interaction increasing with more  $s$  character at the bridging carbon. Similarly, larger, more diffuse  $\pi$ -systems in the bridging ligands increase their polarizability, affording additional polarization stabilization. Finally, the ionic character of the interaction is embodied in the charge-transfer component, for which a similar trend is observed. As expected, the heteroatom bridging ligand exhibits the largest charge-transfer stabilization. Overall, the  $Cu_2-C$  bonds are primarily covalent, which may explain why treatment with excess water does not immediately hydrolyze 1 and why exchange of the  $\mu$ -Me ligand for pentafluorophenyl is sluggish. In contrast, the computations suggest that the pentafluorophenoxide complex has no covalent stabilization, and its interaction is almost exclusively due to charge transfer, with some polarization, suggesting that the  $Cu_2-O$  bond in 5 is primarily ionic.

## CONCLUDING REMARKS

These results demonstrate that a dicopper core can support bridging alkyl ligands, and the resulting complexes are unexpectedly persistent in solution. Upon treatment with suitably acidic reagents, the bridging methyl was exchanged for other bridging ligands. In addition, the dicopper  $\mu$ -methyl complex was found to undergo facile alkyl-aryl exchange with  $BPh_3$ , affording a dicopper  $\mu$ -phenyl complex. However, no insertion into the dicopper-carbon bond was observed with a variety of reagents. Electrochemical characterization revealed a reversible oxidation-reduction event for the  $\mu$ -methyl complex and a quasireversible event for the  $\mu$ -neopentyl derivative, evidencing the existence of transient mixed-valence dicopper alkyl complexes.

The dicopper(I,I) alkyl complexes extend a series of hydrocarbyl fragments bridging two copper centers, allowing for comparisons of binding through  $sp^3$ ,  $sp^2$ , and  $sp$ -hybridized carbon atoms. Notably, structural comparisons show that the  $Cu-C$  distances shorten and  $\angle Cu-C-Cu$  angles widen with increasing  $s$  character at the bridging carbon. Measurements of the complexes' oxidation potentials reveal the  $\mu$ -alkyl complexes to be significantly more reducing than the  $\mu$ -aryl and  $\mu$ -alkynyl complexes. Computational decomposition of bonding contributions suggests that the dicopper-carbon bonds are primarily covalent in nature, possibly contributing to their relative persistence.

This work further extends the study of discrete cationic dicopper complexes containing bridging organic ligands. Notably, the reactivity profile observed suggests that these dicopper alkyl complexes contain a new type of organocopper moiety that could enable yet undiscovered reaction pathways. We further expect that the  $[Cu_2(DPFN)]^{2+}$  platform could serve to support a range of other reactive fragments and enable fundamental studies of their structure and reactivity. These studies could aid the discovery of new reagents and catalysts and help elucidate mechanisms of reactions that occur at a dicopper core.

## EXPERIMENTAL SECTION

**General Considerations.** Unless otherwise stated, all reactions and manipulations were carried out under a dry nitrogen atmosphere employing either standard Schlenk techniques or VAC Atmospheres or MBRAUN gloveboxes.

Pentane (HPLC grade), toluene (ACS grade), and acetonitrile (HPLC grade) were purchased from Fischer Scientific. Diethyl ether (HPLC grade) and dichloromethane (HPLC grade) were purchased from Honeywell. Hexanes (HPLC grade) was purchased from JT Baker. Tetrahydrofuran (THF) (ChromAR) were purchased from Macron Fine Chemicals, and *o*-difluorobenzene ( $o-C_6H_4F_2$ ) was purchased from Oakwood. Pentane, toluene, diethyl ether, tetrahydrofuran, acetonitrile, dichloromethane, and *o*-difluorobenzene were dried and deaerated using a JC Meyers Phoenix SDS solvent purification system. Hexanes were dried and deaerated using a VAC Atmospheres solvent purification system. Nitrobenzene- $d_5$  ( $C_6D_5NO_2$ ) was purchased from Cambridge Isotope Laboratories. Tetrahydrofuran- $d_8$

Table 4. Bonded Energy Decomposition Analysis of the Interaction between  $[Cu_2(DPFN)]^{2+}$  and Various Bridging Ligands

	energy component (kcal/mol)			
	$\mu$ -methyl	$\mu$ -phenyl	$\mu$ -phenylalkynyl	$\mu$ -pentafluorophenoxide
preparation and frozen	128.9	141.8	202.8	17.4
spin-coupling	-175.8	-176.3	-216.5	0.0
polarization	-18.7	-20.3	-74.7	-26.5
charge-transfer	-33.0	-59.1	-61.1	-141.6
total energy	-98.6	-114.0	-149.5	-150.6

(THF- $d_8$ ) was purchased from Cambridge Isotope Laboratories (D, 99.5%) or Aldrich (99.5 atom % D). Nitrobenzene- $d_5$  was degassed by three freeze–pump–thaw cycles and stored in the dark, under nitrogen, over 3 Å molecular sieves. Tetrahydrofuran- $d_8$  was degassed by three freeze–pump–thaw cycles and stored in the dark, under nitrogen over 3 Å molecular sieves. Deaerated water was obtained from a Millipore Milli-Q water purification system, sparged with nitrogen for 24 h, and stored in a PTFE-valved flask. All other solvents were obtained from commercial suppliers, distilled or transferred under reduced pressure from appropriate drying reagents, and stored in PTFE-valved flasks.

The ligand 2,7-bis(fluoro-di(2-pyridyl)methyl)-1,8-naphthyridine (DPFN) and dicopper complexes  $[\text{Cu}_2(\mu\text{-}\eta^1\text{-}\eta^1\text{-NCCH}_3\text{)DPFN}] (\text{NTf}_2)_2$ ,  $[\text{Cu}_2(\mu\text{-}\eta^1\text{-}\eta^1\text{-Ph)DPFN}] \text{NTf}_2$ , and  $[\text{Cu}_2(\mu\text{-}\eta^1\text{-}\eta^1\text{-C}\equiv\text{C}(\text{C}_6\text{H}_4)\text{CH}_3\text{)DPFN}] \text{NTf}_2$  were synthesized as previously reported.<sup>25,26</sup> Additional spectroscopic data for the first three of these compounds are reported in the Supporting Information. The internal standard 1,3,5-tris(trifluoromethyl)benzene was degassed by three freeze–pump–thaw cycles and stored under nitrogen over 3 Å molecular sieves. Tetrabutylammonium hexafluorophosphate ( $[\text{tBu}_4\text{N}][\text{PF}_6]$ , 99.0+%) was obtained from Fluka and dried in vacuo. Methylolithium, as a 1.6 M solution in diethyl ether, was purchased from Aldrich and stored at  $-30\text{ }^\circ\text{C}$ . Triflimidic acid (95+%) was purchased from Matrix Scientific. Dimethylmagnesium was synthesized via dioxane addition to methylmagnesium bromide,<sup>88</sup> and before use a solution of the product in THF was titrated by  $^1\text{H}$  NMR spectroscopy.<sup>89</sup> Diethylmagnesium was synthesized and titrated similarly. Neopentylolithium was synthesized in the usual manner<sup>90</sup> by heating a mixture of lithium dispersion with high-sodium ( $\sim 1.0\%$ ) content and deoxygenated neopentyl chloride,<sup>91</sup> filtering, and recrystallizing the product from a concentrated pentane solution cooled to  $-30\text{ }^\circ\text{C}$ . Ethyllithium, as a 0.5 M solution in benzene/cyclohexane, was purchased from Sigma-Aldrich. Sodium tetraethylborate (97%) was obtained from Aldrich. Lithium chloride was dried in vacuo at  $210\text{ }^\circ\text{C}$  for 12 h. Pentafluorophenol ( $\geq 99\%$ ) and triphenylborane were obtained from Aldrich and used as received. Carbon dioxide (4.8, research grade) was obtained from Praxair, and 1-hexene was deaerated by three freeze–pump–thaw cycles and stored over molecular sieves.

Unless otherwise noted, all other liquid reagents were obtained from commercial suppliers, distilled or transferred under reduced pressure from appropriate drying reagents, and stored under nitrogen while all other solid reagents were obtained from commercial suppliers and used without further purification.

**Analytical Methods.** Carbon, hydrogen, and nitrogen elemental analyses were performed by the College of Chemistry's Microanalytical Facility at the University of California, Berkeley.

**NMR Spectroscopy.** Unless otherwise stated, NMR spectra were acquired between 294 and 299 K using Bruker AV-400, DRX-500, AV-500, AV-600, and AV-700 spectrometers.  $^1\text{H}$  NMR spectra were referenced to tetramethylsilane via residual solvent peaks ( $\delta$  8.11 for  $\text{C}_6\text{D}_5\text{NO}_2$ ,  $\delta$  3.58 for THF- $d_8$ ), while  $^{13}\text{C}\{^1\text{H}\}$  NMR spectra were referenced via solvent resonances ( $\delta$  148.6 for  $\text{C}_6\text{D}_5\text{NO}_2$ ,  $\delta$  67.21 for THF- $d_8$ ).<sup>92</sup> In deuterated solvents,  $^{19}\text{F}$  NMR spectra were internally referenced to the 1,3,5-tris(trifluoromethyl)benzene resonance ( $\delta$   $-62.73$  ppm vs  $\text{CFCl}_3$  in  $\text{C}_6\text{D}_5\text{NO}_2$  at  $23\text{ }^\circ\text{C}$ ,  $\delta$   $-62.97$  ppm vs  $\text{CFCl}_3$  in THF- $d_8$  at  $22\text{ }^\circ\text{C}$ ), which was in turn referenced to dissolved  $\text{CFCl}_3$ , which was set to 0.00 ppm. Spectra of compounds dissolved in neat *o*-difluorobenzene were obtained without lock and by automatic gradient shimming on the solvent resonances in the proton spectrum or by manually shimming on the FID. For  $^1\text{H}$  NMR spectroscopy, these spectra were referenced to tetramethylsilane (via a solvent resonance), and for  $^{19}\text{F}$  NMR spectroscopy, these spectra were referenced to  $\text{CFCl}_3$  through either 1,3,5-tris(trifluoromethyl)benzene ( $\delta$   $-63.58$  ppm vs  $\text{CFCl}_3$  in *o*-difluorobenzene at  $23\text{ }^\circ\text{C}$ ) or the solvent fluorine resonance ( $\delta$   $-138.91$  ppm vs  $\text{CFCl}_3$  in *o*-difluorobenzene at  $23\text{ }^\circ\text{C}$ ). Similarly, spectra of compounds in THF- $H_8$  were obtained without lock and by shimming as described above. For  $^1\text{H}$  NMR spectroscopy, they were referenced to tetramethylsilane (via a solvent resonance), and for  $^{19}\text{F}$  NMR spectroscopy they were referenced to  $\text{CFCl}_3$  via 1,3,5-tris(trifluoromethyl)benzene ( $\delta$   $-62.91$  ppm vs  $\text{CFCl}_3$

in THF- $H_8$  at  $23\text{ }^\circ\text{C}$ ).  $^{11}\text{B}\{^1\text{H}\}$  spectra were referenced to the IUPAC-recommended unified scale (reference compound  $\text{BF}_3\cdot\text{Et}_2\text{O}$  in  $\text{CDCl}_3$ )<sup>93</sup> employing the samples' tetramethylsilane-referenced  $^1\text{H}$  NMR spectra and the Absolute Reference tool in MestReNova (v. 10.0.2).  $^2\text{H}\{^1\text{H}\}$  spectra were similarly referenced to the unified scale (reference compound: neat  $\text{Si}(\text{CD}_3)_4$ ). Temperatures were calibrated using methanol (4% in methanol- $d_4$ ) standards. All coupling constants are reported as absolute values.

Spectra recorded at 21.1 T were acquired with a 5 mm CPTCI 1H-13C/15N/D Z-GRD Z44910 probe. Spectra recorded at 16.4 T were acquired with a 5 mm CPTXI 1H-13C/15N/D Z-GRD Z44906 probe. Spectra recorded at 14.1 T were acquired with a 5 mm PABBO BB-1H/D Z-GRD Z847801 probe. Spectra recorded at 11.7 T were acquired with a 5 mm TBI 1H/31P/D-BB Z-GRD Z8641 probe. Spectra recorded at 9.40 T were acquired with a 5 mm QNP 1H/13C/31P/19F Z-GRD Z8400 probe.

For the bridging methyl and neopentyl ligands in complexes **1** and **3**, respectively, one-bond carbon–hydrogen coupling constants ( $^1J_{\text{C-H}}$ ) were determined from the  $^{13}\text{C}$  satellite peaks directly observed in  $^1\text{H}$  NMR spectra. When possible for ligand resonances in complex **1** and for the bridging ethyl resonances in **4**, carbon–hydrogen coupling constants were measured from satellites observed in  $^1\text{H}$ – $^{13}\text{C}$  HMBC spectra.

Proton-coupled  $^1\text{H}$ – $^{13}\text{C}$  HSQC spectra of complex **1** were obtained at 16.4 T and 298 K by employing a modified hsqcctgspis2.2 pulse sequence in which the  $^1\text{H}$  refocusing pulse during the  $t_1$  evolution period was omitted and replaced with a delay. The  $^1J$  coupling constant (CNST2) was set to 115.8 Hz. Standard  $^1\text{H}$ – $^{13}\text{C}$  HSQC spectra of complex **1** were also obtained at 16.4 T and 298 K.

All NMR spectra were analyzed and spin simulations were performed with MestReNova (v. 10.0.2). Spectra included in the Supporting Information were annotated using Adobe Illustrator CS6.

**IR Spectroscopy.** Infrared spectra were recorded with a Bruker Vertex 80 FTIR spectrometer with a room-temperature DLaTGS detector using OPUS software (v. 7.2) and employing an A225/Q Platinum ATR accessory. All measurements were made at  $4.0\text{ cm}^{-1}$  resolution. Spectra included in the Supporting Information were plotted in Microsoft Excel 2016.

**UV–Visible Spectroscopy.** Samples for UV–visible spectrophotometry were prepared in a nitrogen-filled glovebox and sealed in 1 cm, air-free quartz cells. UV–visible spectra were obtained on a Shimadzu UV-2450 UV–visible spectrophotometer using UVProbe software (v. 2.21).

**X-ray Crystallography.** X-ray diffraction data for complexes **2**, **3**, **5**, and **6** were collected using a Bruker AXS diffractometer with a Kappa geometry goniostat coupled to an APEX-II CCD detector with  $\text{Mo K}\alpha$  ( $\lambda = 0.71073\text{ \AA}$ ) radiation generated by a microfocus sealed tube and monochromated by a system of QUAZAR multilayer mirrors. Data for complexes **1** and **4** were collected at Beamline 11.3.1 of the Advanced Light Source at Lawrence Berkeley National Laboratory using a Bruker D8 diffractometer coupled to a Photon 100 detector with  $\text{Si}(111)$ -monochromated synchrotron radiation ( $16\text{ keV}$ ,  $\lambda = 0.7749\text{ \AA}$ ). Unless otherwise noted, crystals were kept at 100(2) K throughout collection. Data collection strategy determination, integration, scaling, and space group determination were performed with Bruker APEX2 (v. 2014.11-0) or APEX3 (v. 2016.5-0) software. Structures were solved with SHELXT-2014 and refined with SHELXL-2014 or SHELXL-2018, with refinement of  $F^2$  on all data by full-matrix least squares.<sup>94,95</sup> The 3D molecular structure figures were visualized with ORTEP 3.2 and annotated with Adobe Illustrator CS6. Disordered cation, anion, and solvent molecules observed in the crystal structures were modeled atomistically. In addition to disordered anions and THF molecules, the structure of complex **4** contained a void partially occupied by other highly disordered solvent molecules, likely diethyl ether. SQUEEZE was employed to treat electron density in the void as a diffuse solvent contribution to the calculated structure factors.<sup>96</sup> Average bond distances and angles computed for complex **3** only incorporate the primary components of the disordered neopentyl groups. Additional details of each experiment

can be found in Table S1 in the Supporting Information and crystallographic information files.

**Electrochemistry.** All electrochemical experiments were performed inside an MBRAUN glovebox using a pass-through consisting of gold-plated tellurium copper binding posts connected to tinned copper conductors shielded with Beldfoil and tinned copper braid. Experiments employed a glassy-carbon working electrode (polished with 0.30 and then 0.05  $\mu\text{m}$  alumina slurries, rinsed with water, and dried in vacuo), a platinum-wire counter electrode, and a Ag/AgNO<sub>3</sub> reference electrode (0.1 M [<sup>109</sup>Bu<sub>4</sub>N][PF<sub>6</sub>], AgNO<sub>3</sub> (saturated) in THF (or *o*-C<sub>6</sub>H<sub>4</sub>F<sub>2</sub> for [Cu<sub>2</sub>( $\mu$ - $\eta^1$ : $\eta^1$ -C $\equiv$ C(C<sub>6</sub>H<sub>4</sub>)CF<sub>3</sub>)DPFN](NTf<sub>2</sub>)) constructed and measured against [Cp<sub>2</sub>Fe]<sup>0/+</sup> immediately before use). Measurements were made with a BASi EC Epsilon potentiostat/galvanostat and a PWR-3 Power Module. Sweep direction and scan rates are included in the relevant figures or their captions. Cyclic voltammograms were recorded in a 0.1 M [<sup>109</sup>Bu<sub>4</sub>N][PF<sub>6</sub>] solution in *o*-difluorobenzene at 22 °C with software-determined *iR* compensation applied. Data analysis, including peak finding and baseline determination employing linear regression, was performed with EC-Lab (v. 10.40).

**General Computational Details.** All calculations were performed with QChem (v. 5.0.1).<sup>97</sup> Starting from the crystallographically determined atomic coordinates of the relevant complexes, the anions and cocrystallized solvent molecules were deleted, and the geometries of the cations were optimized. Visualizations were performed with the IQmol software package.<sup>98</sup>

**IR Frequency Calculations.** Calculations employed the  $\omega$ B97X-D functional<sup>42</sup> and the def2-TZVP basis set for all atoms and used a (99,590) integration grid. As the electronic structure calculation is approximate and anharmonic effects were not included, the frequencies were then scaled by 0.95.<sup>99,100</sup> The broadened spectrum was simulated with Gaussian line shapes overlaid on an impulse representation of the frequencies and their intensities.

**Energy Decomposition Analysis.** Calculations employed the  $\omega$ B97X-D functional<sup>42</sup> and the def2-SVP basis set for all atoms and used a (99,590) integration grid. Energy decomposition analysis (EDA) was carried out as described previously,<sup>86,87</sup> with the final energy scaled as described therein. Though previous reports using this EDA were concerned primarily with single bonds between pairs of atoms, the method can be applied to any system in which one pair of electrons becomes uncoupled when the bond is ruptured. In this three-center, two-electron (3c–2e) system, the interacting fragments are a doublet alkyl component and a doublet dicopper–DPFN component that interact to form the 3c–2e bond of interest. For example, for complex 1 the two components employed were CH<sub>3</sub><sup>•</sup> and Cu<sub>2</sub>DPFN<sup>•+</sup>.

**Synthesis of [Cu<sub>2</sub>( $\mu$ - $\eta^1$ : $\eta^1$ -CH<sub>3</sub>)DPFN](NTf<sub>2</sub>) (1).** *Method 1.* A solution of [Cu<sub>2</sub>( $\mu$ - $\eta^1$ : $\eta^1$ -NCCH<sub>3</sub>)DPFN](NTf<sub>2</sub>)<sub>2</sub> (0.050 g, 0.041 mmol) in THF (2.0 mL) was cooled to –30 °C; to the cold stirred solution was added a solution of dimethylmagnesium in THF (0.5 mL, 41 mM, 0.021 mmol, 0.51 equiv) dropwise. The reaction mixture darkened significantly and was stirred rapidly for 1 h while it was warmed to room temperature (ca. 22 °C). The resulting mixture was filtered, and the filtrate was cooled to –30 °C. Diethyl ether (approximately 17 mL) was layered over the cold filtrate. After 2 days at –35 °C, a dark solid formed, and the dark red supernatant was carefully decanted. The solid was briefly triturated with diethyl ether (3  $\times$  2 mL). The resulting solid was suspended in 4 mL of diethyl ether and transferred to a new vial. After the solid was allowed to settle, the supernatant was carefully decanted; residual volatile compounds were removed in vacuo to yield 1 as an olive green powder (0.019 g, 0.021 mmol, 51%). For long-term storage, the product was kept under nitrogen at –35 °C and in the dark. Vapor diffusion of diethyl ether into a *o*-C<sub>6</sub>H<sub>4</sub>F<sub>2</sub> solution of 1, synthesized employing dimethylmagnesium, for 14 days at –35 °C afforded X-ray-quality crystals of 1 suitable for diffraction on a Bruker AXS diffractometer with Mo K $\alpha$  radiation.

*Method 2.* A solution of [Cu<sub>2</sub>( $\mu$ - $\eta^1$ : $\eta^1$ -NCCH<sub>3</sub>)DPFN](NTf<sub>2</sub>)<sub>2</sub> (0.050 g, 0.041 mmol) in THF (2.5 mL) was cooled to –30 °C; to the cold stirred solution was added a similarly cold solution of

methylithium in diethyl ether (28  $\mu\text{L}$ , 1.6 M, 1.1 equiv) dropwise. The red solution became dark and was stirred for 35 min as the reaction mixture was warmed to room temperature. The resulting mixture was filtered, and the filtrate was cooled to –30 °C. Diethyl ether (approximately 18 mL) was layered over the cold filtrate. After 2 days at –35 °C, a dark crystalline solid formed, and the supernatant was carefully decanted. The solid was briefly rinsed with diethyl ether (5  $\times$  1 mL), and residual volatile compounds were removed in vacuo to yield 1 as a dark crystalline solid (0.024 g, 0.026 mmol, 63%). Crystals obtained from the aforementioned steps were suitable for diffraction employing synchrotron radiation at Beamline 11.3.1 at the LBNL Advanced Light Source. Depending on the quality of the methylithium solution used, the product sometimes contained a small percentage (ca.  $\leq$ 5%) of the bridging chloride complex (2), as determined by <sup>1</sup>H and <sup>19</sup>F NMR spectroscopy. <sup>1</sup>H NMR (700.13 MHz, THF-*d*<sub>6</sub>):  $\delta$  8.83 (ddd, *J* = 5.0, 1.7, 0.9 Hz, 4H, 6-pyridyl-C–H), 8.77 (d, *J* = 8.5 Hz, 2H, 4-naphth-C–H), 8.37 (dd, *J* = 8.5, 3.1 Hz, 2H, 3-naphth-C–H), 8.13 (ddt, *J* = 8.1, 3.4, 1.1 Hz, 4H, 3-pyridyl-C–H), 8.02 (td, *J* = 7.9, 1.7 Hz, 4H, 4-pyridyl-C–H), 7.51 (ddd, *J* = 7.6, 5.0, 1.1 Hz, 4H, 5-pyridyl-C–H), 0.89 (s, 3H, Cu<sub>2</sub>–CH<sub>3</sub>, *J*<sub>C–H</sub> = 115.8 Hz). <sup>1</sup>H NMR (600.13 MHz, THF-*d*<sub>8</sub>):  $\delta$  8.83 (ddd, *J* = 5.1, 1.9, 1.0 Hz, 4H), 8.77 (d, *J* = 8.6 Hz, 2H), 8.37 (dd, *J* = 8.6, 3.1 Hz, 2H), 8.13 (ddt, *J* = 8.2, 3.4, 1.1 Hz, 4H), 8.02 (td, *J* = 7.9, 1.7 Hz, 4H), 7.51 (ddd, *J* = 7.6, 5.0, 1.2 Hz, 4H), 0.89 (s, 3H, *J*<sub>C–H</sub> = 115.8 Hz). <sup>13</sup>C{<sup>1</sup>H} NMR (150.92 MHz, THF-*d*<sub>6</sub>):  $\delta$  159.80 (d, *J* = 30.3 Hz, 2-naphth-C), 154.27 (d, *J* = 29.2 Hz, 2-pyridyl-C), 150.85 (8a-naphth-C), 149.87 (d, *J* = 3.0 Hz, 6-pyridyl-C–H, *J*<sub>C–H</sub> = 183.3 Hz), 140.79 (d, *J* = 3.3 Hz, 4-naphth-C–H, *J*<sub>C–H</sub> = 169.7 Hz), 139.32 (d, *J* = 3.3 Hz, 4-pyridyl-C–H, *J*<sub>C–H</sub> = 167.6 Hz), 125.19 (5-pyridyl-C–H), 123.61 (4a-naphth-C), 121.08 (d, <sup>101</sup>*J* = 322.6 Hz, –SO<sub>2</sub>–CF<sub>3</sub>), 120.87 (d, *J* = 14.1 Hz, 3-pyridyl-C–H), 119.85 (d, *J* = 14.6 Hz, 3-naphth-C–H, *J*<sub>C–H</sub> = 172.4 Hz), 94.41 (d, *J* = 185.4 Hz, (pyridyl)<sub>2</sub>(naphth)C–F), –40.22 (br, Cu<sub>2</sub>–CH<sub>3</sub>). <sup>19</sup>F NMR (564.61 MHz, THF-*d*<sub>6</sub>):  $\delta$  –79.03 (s, 6F, –SO<sub>2</sub>–CF<sub>3</sub>), –174.31 (q, <sup>102</sup>*J* = 3.5 Hz, 2F, (pyridyl)<sub>2</sub>(naphth)C–F). <sup>1</sup>H NMR (499.60 MHz, THF-*H*<sub>8</sub>):  $\delta$  8.83 (d, *J* = 5.0 Hz, 4H), 8.77 (d, *J* = 8.6 Hz, 2H), 8.37 (dd, *J* = 8.5, 3.1 Hz, 2H), 8.12 (dd, *J* = 8.2, 3.4 Hz, 4H), 8.01 (td, *J* = 7.8, 1.7 Hz, 4H), 7.50 (dd, *J* = 7.6, 4.9 Hz, 4H), 0.89 (s, 3H). <sup>19</sup>F NMR (564.61 MHz, THF-*H*<sub>8</sub>):  $\delta$  –79.01 (6F), –174.32 (2F). <sup>1</sup>H NMR (600.13 MHz, *o*-C<sub>6</sub>H<sub>4</sub>F<sub>2</sub>):  $\delta$  8.77 (dd, *J* = 4.9, 1.7 Hz, 4H), 8.22 (d, *J* = 8.5 Hz, 2H), 8.11 (dd, *J* = 8.6, 3.0 Hz, 2H), 7.95 (dd, *J* = 8.2, 3.3 Hz, 4H), 7.74 (td, *J* = 7.9, 1.7 Hz, 4H), 7.24 (dd, *J* = 7.6, 5.0 Hz, 4H), <sup>103</sup>1.05 (s, 3H). <sup>19</sup>F NMR (564.61 MHz, *o*-C<sub>6</sub>H<sub>4</sub>F<sub>2</sub>):  $\delta$  –78.54 (s, 6F), –175.13 (q, *J* = 3.5 Hz, 2F). IR (ATR,  $\tilde{\nu}$  (cm<sup>–1</sup>)): 3124 (vw, br), 3066 (vw), 2978 (vw, br), 2859 (vw), 2781 (vw), 1605 (w, sh), 1592 (m), 1575 (w), 1546 (vw), 1500 (w), 1472 (w, sh), 1462 (m), 1439 (w), 1410 (w), 1349 (s), 1331 (m), 1302 (w, sh), 1294 (w), 1240 (w), 1228 (w), 1179 (vs), 1146 (m, sh), 1134 (vs), 1096 (w), 1074 (m), 1061 (s), 1008 (w), 977 (vw, br), 941 (vw), 927 (vw), 903 (vw), 891 (vw), 855 (m), 807 (w), 787 (m), 773 (s), 752 (m), 737 (m), 711 (w), 698 (m), 686 (m), 651 (m), 642 (m), 620 (m), 597 (s), 582 (m), 569 (s), 532 (w), 507 (s), 442 (vw, br), 430 (vw), 413 (m). UV–vis (THF)  $\lambda_{\text{max}}$ , nm ( $\epsilon$ , M<sup>–1</sup> cm<sup>–1</sup>/10<sup>3</sup>): 253 (18.3), 295 (12.8), 306 (sh 10.8), 318 (10.8), 347 (sh 4.34), 404 (2.72), 635 (0.404). Anal. Calcd for C<sub>33</sub>H<sub>23</sub>Cu<sub>2</sub>F<sub>8</sub>N<sub>7</sub>O<sub>4</sub>S<sub>2</sub>: C, 42.86; H, 2.51; N, 10.60. Found: C, 42.50; H, 2.70; N, 10.27. IR, UV–vis, elemental analysis, and cyclic voltammetry (Figures S19–S22) were performed using samples prepared by Method 1.

**Synthesis of [Cu<sub>2</sub>( $\mu$ -Cl)DPFN](NTf<sub>2</sub>) (2).** To a stirred solution of [Cu<sub>2</sub>( $\mu$ - $\eta^1$ : $\eta^1$ -NCCH<sub>3</sub>)DPFN](NTf<sub>2</sub>)<sub>2</sub> (0.050 g, 0.041 mmol) in THF (2 mL) was added a solution of anhydrous lithium chloride in THF (1.0 mL, 0.041 M, 0.041 mmol, 1.0 equiv) dropwise. The reaction mixture rapidly became dark red and was stirred for 1.25 h. The mixture was then filtered, and the filtrate was collected and concentrated in vacuo. The resulting dark red-purple oil was triturated by rapid stirring with diethyl ether (4 mL) for 1 h. The solid was allowed to settle, and the supernatant was carefully decanted. The solid was similarly triturated twice more with diethyl ether (4 mL for 1 h each time). The resulting solid was rinsed briefly with diethyl ether (4 mL), and residual volatile compounds were removed in vacuo to yield 2 as

a dark gray solid (0.035 g, 0.037 mmol, 90%). Layering of diethyl ether over a cold ( $-30\text{ }^{\circ}\text{C}$ ), dilute solution of **2** in THF and storage for 2 days at  $-35\text{ }^{\circ}\text{C}$  afforded X-ray-quality crystals of  $2\cdot\text{C}_4\text{H}_8\text{O}$ .  $^1\text{H}$  NMR (700.13 MHz, THF- $d_6$ ):  $\delta$  8.90 (dt,  $J = 5.0, 0.8$  Hz, 4H, 6-pyridyl-C-H), 8.89 (d,  $J = 8.6$  Hz, 2H, 4-naphth-C-H), 8.47 (dd,  $J = 8.6, 3.2$  Hz, 2H, 3-naphth-C-H), 8.16 (ddt,  $J = 8.2, 3.4, 1.1$  Hz, 4H, 3-pyridyl-C-H), 8.05 (td,  $J = 7.9, 1.8$  Hz, 4H, 4-pyridyl-C-H), 7.54 (ddd,  $J = 7.6, 5.0, 1.1$  Hz, 4H, 5-pyridyl-C-H).  $^{13}\text{C}\{^1\text{H}\}$  NMR (150.92 MHz, THF- $d_6$ ):  $\delta$  160.18 (d,  $J = 30.0$  Hz, 2-naphth-C), 153.85 (d,  $J = 29.7$  Hz, 2-pyridyl-C), 150.20 (8a-naphth-C), 149.78 (d,  $J = 3.0$  Hz, 6-pyridyl-C-H), 141.67 (d,  $J = 3.5$  Hz, 4-naphth-C-H), 139.67 (d,  $J = 3.3$  Hz, 4-pyridyl-C-H), 125.33 (5-pyridyl-C-H), 124.14 (4a-naphth-C), 121.08 (d,  $J = 14.1$  Hz, 3-pyridyl-C-H), 121.04 (q,  $J = 322.4$  Hz,  $-\text{SO}_2-\text{CF}_3$ ), 120.46 (d,  $J = 16.3$  Hz, 3-naphth-C-H), 93.79 (d,  $J = 186.6$  Hz, (pyridyl) $_2$ (naphth)C-F).  $^{19}\text{F}$  NMR (564.61 MHz, THF- $d_6$ ):  $\delta$  -79.05 (s, 6F,  $-\text{SO}_2-\text{CF}_3$ ), -172.83 (q,  $^{104}J = 3.5$  Hz, 2F, (pyridyl) $_2$ (naphth)C-F).  $^1\text{H}$  NMR (499.60 MHz, THF- $H_8$ ):  $\delta$  8.90 (d,  $J = 5.1$  Hz, 4H), 8.88 (d,  $J = 8.7$  Hz, 2H), 8.46 (dd,  $J = 8.6, 3.3$  Hz, 2H), 8.15 (dd,  $J = 8.3, 3.4$  Hz, 4H), 8.05 (t,  $J = 7.4$  Hz, 4H), 7.54 (dd,  $J = 7.7, 5.0$  Hz, 4H).  $^1\text{H}$  NMR (600.13 MHz,  $o\text{-C}_6\text{H}_4\text{F}_2$ ):  $\delta$  8.90 (d,  $J = 5.0$  Hz, 4H), 8.34 (d,  $J = 8.6$  Hz, 2H), 8.22 (dd,  $J = 8.6, 3.0$  Hz, 2H), 7.98 (dd,  $J = 8.2, 3.3$  Hz, 4H), 7.76 (td,  $J = 7.9, 1.7$  Hz, 4H), 7.24 (dd,  $J = 7.6, 4.9$  Hz, 4H).  $^{19}\text{F}$  NMR (564.61 MHz,  $o\text{-C}_6\text{H}_4\text{F}_2$ ):  $\delta$  -78.57 (s, 6F), -173.65 (q,  $J = 3.5$  Hz, 2F). IR (ATR,  $\tilde{\nu}$  ( $\text{cm}^{-1}$ )): 3130 (vw, br), 3074 (vw), 3057 (vw), 1603 (w, sh), 1593 (m), 1575 (w), 1544 (vw), 1502 (w), 1472 (w, sh), 1463 (m), 1439 (w), 1426 (w, sh), 1407 (vw), 1350 (s), 1333 (m), 1303 (w), 1293 (w), 1241 (w, sh), 1228 (w), 1181 (vs), 1136 (vs), 1096 (w), 1075 (m), 1062 (s), 1012 (w), 1001 (w, sh), 979 (vw), 968 (vw), 941 (vw), 928 (vw), 902 (vw), 891 (vw), 858 (m), 807 (w), 787 (m), 773 (s), 765 (m, sh), 751 (m), 738 (m), 711 (w), 699 (w), 686 (m), 652 (m), 646 (m), 619 (m), 596 (s), 581 (m), 569 (s), 532 (w), 507 (s), 456 (vw), 419 (w), 413 (w). UV-vis (THF)  $\lambda_{\text{max}}$  nm ( $\epsilon$ ,  $\text{M}^{-1}\text{cm}^{-1}/10^3$ ): 252 (20.6), 261 (20.6), 280 (sh 16.5), 308 (14.9), 317 (15.3), 378 (3.93), 531 (0.932), 719 (sh 0.218). Anal. Calcd for  $\text{C}_{32}\text{H}_{20}\text{ClCu}_2\text{F}_8\text{N}_7\text{O}_4\text{S}_2$ : C, 40.66; H, 2.13; N, 10.37. Found: C, 40.29; H, 2.22; N, 10.31.

**Synthesis of  $[\text{Cu}_2(\mu\text{-}\eta^1\text{-}\eta^1\text{-CH}_2\text{C}(\text{CH}_3)_3)\text{DPFN}]\text{NTf}_2$  (**3**).** A solution of  $[\text{Cu}_2(\mu\text{-}\eta^1\text{-}\eta^1\text{-NCCH}_3)\text{DPFN}](\text{NTf}_2)_2$  (0.0400 g, 0.032 mmol) in THF (3 mL) was cooled to  $-30\text{ }^{\circ}\text{C}$ . To the stirred solution was added a solution of neopentylolithium (0.0027 g, 0.034 mmol) in pentane (0.75 mL) dropwise, resulting in a darkening of the reaction mixture. The mixture was stirred for an additional 50 min while it was warmed to room temperature and then filtered. The filtrate was collected and cooled to ca.  $-35\text{ }^{\circ}\text{C}$ , and diethyl ether (approximately 17 mL) was layered over the cold filtrate. Dark crystalline solid formed after storage for 2 days at  $-35\text{ }^{\circ}\text{C}$ . The supernatant was carefully decanted, and the solid was washed with diethyl ether ( $4 \times 1$  mL). Residual volatile compounds were removed in vacuo to yield **3** as a dark crystalline solid (0.016 g, 0.016 mmol, 50%). The product was stored under nitrogen at  $-35\text{ }^{\circ}\text{C}$  and in the dark. Vapor diffusion of diethyl ether into a THF solution of **3** for 7 days at  $-35\text{ }^{\circ}\text{C}$  afforded X-ray-quality crystals of  $3\cdot\text{C}_4\text{H}_8\text{O}$ .  $^1\text{H}$  NMR (700.13 MHz, THF- $d_6$ ):  $\delta$  8.95 (dd,  $J = 5.1, 1.6$  Hz, 4H, 6-pyridyl-C-H), 8.79 (d,  $J = 8.5$  Hz, 2H, 4-naphth-C-H), 8.38 (dd,  $J = 8.6, 3.1$  Hz, 2H, 3-naphth-C-H), 8.08 (ddt,  $J = 8.1, 2.4, 1.1$  Hz, 4H, 3-pyridyl-C-H), 8.03 (td,  $J = 7.9, 1.8$  Hz, 4H, 4-pyridyl-C-H), 7.55 (ddd,  $J = 7.5, 5.0, 1.3$  Hz, 4H, 5-pyridyl-C-H), 1.93 (s, 2H,  $\text{Cu}_2\text{-CH}_2\text{C}(\text{CH}_3)_3$ ,  $J_{\text{C-H}} = 107.4$  Hz), 1.36 (s, 9H,  $\text{Cu}_2\text{-CH}_2\text{C}(\text{CH}_3)_3$ ).  $^1\text{H}$  NMR (600.13 MHz, THF- $d_6$ ):  $\delta$  8.95 (ddt,  $J = 5.1, 1.8, 0.9$  Hz, 4H), 8.79 (d,  $J = 8.6$  Hz, 2H), 8.38 (dd,  $J = 8.6, 3.1$  Hz, 2H), 8.08 (ddt,  $J = 8.1, 2.4, 1.1$  Hz, 4H), 8.03 (td,  $J = 7.8, 1.7$  Hz, 4H), 7.55 (ddd,  $J = 7.5, 5.0, 1.3$  Hz, 4H), 1.92 (s, 2H), 1.36 (s, 9H,  $J_{\text{C-H}} = 123.3$  Hz).  $^{13}\text{C}\{^1\text{H}\}$  NMR (150.92 MHz, THF- $d_6$ ):  $\delta$  160.72 (d,  $J = 30.5$  Hz, 2-naphth-C), 155.40 (d,  $J = 28.3$  Hz, 2-pyridyl-C), 151.22 (8a-naphth-C), 150.11 (d,  $J = 2.4$  Hz, 6-pyridyl-C-H), 141.29 (d,  $J = 3.3$  Hz, 4-naphth-C-H), 139.45 (d,  $J = 2.8$  Hz, 4-pyridyl-C-H), 125.39 (5-pyridyl-C-H), 123.69 (4a-naphth-C), 123.21 (d,  $^{101}J = 322.2$  Hz,  $-\text{SO}_2-\text{CF}_3$ ), 121.71 (d,  $J = 13.8$  Hz, 3-pyridyl-C-H), 120.05 (d,  $J = 14.9$  Hz, 3-naphth-C-H), 95.31 (d,  $J = 184.4$  Hz, (pyridyl) $_2$ (naphth)C-F),

37.21 ( $\text{Cu}_2\text{-CH}_2\text{C}(\text{CH}_3)_3$ ), 34.45 ( $\text{Cu}_2\text{-CH}_2\text{C}(\text{CH}_3)_3$ ), 13.02 (br,  $\text{Cu}_2\text{-CH}_2\text{C}(\text{CH}_3)_3$ ).  $^{19}\text{F}$  NMR (564.61 MHz, THF- $d_6$ ):  $\delta$  -79.01 (s, 6F,  $-\text{SO}_2-\text{CF}_3$ ), -166.70 (q,  $^{105}J = 3.0$  Hz, 2F, (pyridyl) $_2$ (naphth)C-F). IR (ATR,  $\tilde{\nu}$  ( $\text{cm}^{-1}$ )): 3111 (vw, br), 3067 (vw, br), 2950 (w), 2928 (w), 2869 (w), 2846 (w), 2812 (vw, br), 2690 (vw, br), 1607 (w), 1592 (m), 1576 (w), 1550 (vw, br), 1502 (w), 1473 (w, sh), 1464 (m), 1438 (m), 1411 (w, br), 1386 (vw), 1350 (s), 1330 (m), 1298 (w), 1241 (w, sh), 1226 (m), 1186 (vs), 1160 (m, sh), 1133 (s), 1101 (vw), 1072 (m, sh), 1055 (s), 1005 (m), 993 (w, sh), 972 (w, br), 942 (vw), 927 (w), 892 (w, br), 856 (m), 808 (m), 773 (s), 753 (m), 739 (m), 711 (w), 699 (m), 686 (m), 652 (m), 640 (m), 618 (s), 599 (m), 570 (s), 510 (m), 483 (m), 453 (w), 430 (w), 416 (m). UV-vis (THF)  $\lambda_{\text{max}}$  nm ( $\epsilon$ ,  $\text{M}^{-1}\text{cm}^{-1}/10^3$ ): 252 (14.7), 295 (9.50), 304 (9.40), 317 (9.10), 343 (sh 4.40), 406 (sh 2.81), 541 (0.633). Anal. Calcd for  $\text{C}_{37}\text{H}_{31}\text{Cu}_2\text{F}_8\text{N}_7\text{O}_4\text{S}_2$ : C, 45.31; H, 3.19; N, 10.00. Found: C, 45.15; H, 3.18; N, 9.85.

**Synthesis of  $[\text{Cu}_2(\mu\text{-}\eta^1\text{-}\eta^1\text{-CH}_2\text{CH}_3)\text{DPFN}]\text{NTf}_2$  (**4**).** A solution of  $[\text{Cu}_2(\mu\text{-}\eta^1\text{-}\eta^1\text{-NCCH}_3)\text{DPFN}](\text{NTf}_2)_2$  (0.020 g, 0.015 mmol) in THF (0.5 mL) was cooled to  $-30\text{ }^{\circ}\text{C}$ ; to the cold stirred solution was added a solution of diethylmagnesium in THF (0.25 mL, 36 mM, 0.0090 mmol, 0.6 equiv). The reaction mixture darkened significantly and was stirred rapidly for 1 h while it was warmed to room temperature (ca.  $22\text{ }^{\circ}\text{C}$ ). The resulting mixture was filtered, and the filtrate was cooled to  $-30\text{ }^{\circ}\text{C}$ . Diethyl ether (approximately 3.25 mL) was layered over the cold filtrate. After 2 days at  $-35\text{ }^{\circ}\text{C}$ , a dark solid formed, and the red supernatant was carefully decanted. The solid was briefly triturated with diethyl ether ( $3 \times 1$  mL). Residual volatile compounds were removed in vacuo to yield a dark solid (0.0085 g). The dark solid was primarily  $[\text{Cu}_2(\mu\text{-}\eta^1\text{-}\eta^1\text{-CH}_2\text{CH}_3)\text{DPFN}]\text{NTf}_2$  (ca.  $\geq 90\%$ , as determined by  $^1\text{H}$  and  $^{19}\text{F}$  NMR spectroscopy). The product was stored at  $-35\text{ }^{\circ}\text{C}$  and in the dark. The aforementioned steps, excluding the removal of volatile compounds in vacuo, provided crystals of  $[\text{Cu}_2(\mu\text{-}\eta^1\text{-}\eta^1\text{-CH}_2\text{CH}_3)\text{DPFN}](\text{NTf}_2)_2\cdot 1.5\text{C}_4\text{H}_8\text{O}\cdot n\text{C}_4\text{H}_{10}\text{O}$  suitable for diffraction, employing synchrotron radiation at Beamline 11.3.1 at the LBNL Advanced Light Source. Numerous attempts to further purify the product by recrystallization from a range of solvent combinations did not provide noticeably purer material, as determined by  $^1\text{H}$  and  $^{19}\text{F}$  NMR spectra.  $^{19}\text{F}$  NMR spectra suggest that the remaining impurities include complexes **2** ( $<2\%$  by  $^{19}\text{F}$  NMR) and **6** ( $<2\%$  by  $^{19}\text{F}$  NMR). Regardless,  $^1\text{H}$ ,  $^{13}\text{C}$ , and  $^{19}\text{F}$  resonances assignable to **4** are easily distinguishable (e.g., see Figures S7–S9) and are reported here  $^1\text{H}$  NMR (700.13 MHz, THF- $d_6$ ):  $\delta$  8.93 (dd,  $J = 5.0, 1.7$  Hz, 4H, 6-pyridyl-C-H), 8.76 (d,  $J = 8.6$  Hz, 2H, 4-naphth-C-H), 8.36 (dd,  $J = 8.5, 3.2$  Hz, 2H, 3-naphth-C-H), 8.14 (dd,  $J = 8.2, 3.2$  Hz, 4H, 3-pyridyl-C-H), 8.03 (td,  $J = 7.9, 1.8$  Hz, 4H, 4-pyridyl-C-H), 7.52 (ddd,  $J = 7.6, 5.0, 1.1$  Hz, 4H, 5-pyridyl-C-H), 2.38 (q,  $J = 7.9$  Hz, 2H,  $\text{Cu}_2\text{-CH}_2\text{CH}_3$ ,  $J_{\text{C-H}} = 111.7$  Hz), 2.14 (t,  $J = 7.9$  Hz, 3H,  $\text{Cu}_2\text{-CH}_2\text{CH}_3$ ,  $J_{\text{C-H}} = 123.2$  Hz).  $^1\text{H}$  NMR (600.13 MHz, THF- $d_6$ ):  $\delta$  8.93 (dd,  $J = 5.1, 1.6$  Hz, 4H), 8.76 (d,  $J = 8.6$  Hz, 2H), 8.36 (dd,  $J = 8.6, 3.1$  Hz, 2H), 8.14 (ddt,  $J = 8.2, 3.4, 1.1$  Hz, 4H), 8.03 (td,  $J = 7.9, 1.7$  Hz, 4H), 7.52 (ddd,  $J = 7.6, 5.0, 1.2$  Hz, 4H), 2.38 (q,  $J = 7.9$  Hz, 2H), 2.14 (t,  $J = 7.9$  Hz, 3H).  $^{13}\text{C}\{^1\text{H}\}$  NMR (150.92 MHz, THF- $d_6$ ):  $\delta$  159.99 (d,  $J = 30.3$  Hz, 2-naphth-C), 154.54 (d,  $J = 29.1$  Hz, 2-pyridyl-C), 150.98 (8a-naphth-C), 150.13 (d,  $J = 3.1$  Hz, 6-pyridyl-C-H), 140.87 (d,  $J = 3.4$  Hz, 4-naphth-C-H), 139.35 (d,  $J = 3.3$  Hz, 4-pyridyl-C-H), 125.19 (5-pyridyl-C-H), 123.65 (4a-naphth-C), 121.00 (d,  $^{101}J = 321.4$  Hz,  $-\text{SO}_2-\text{CF}_3$ ), 120.98 (d,  $J = 14.5$  Hz, 3-pyridyl-C-H), 119.80 (d,  $J = 14.9$  Hz, 3-naphth-C-H), 94.41 (d,  $J = 185.5$  Hz, (pyridyl) $_2$ (naphth)C-F), 19.39 ( $\text{Cu}_2\text{-CH}_2\text{CH}_3$ ), -21.22 (br,  $\text{Cu}_2\text{-CH}_2\text{CH}_3$ ).  $^{19}\text{F}$  NMR (564.61 MHz, THF- $d_6$ ):  $\delta$  -78.99 (s,  $-\text{SO}_2-\text{CF}_3$ ), -173.08 (q,  $^{106}J = 3.4$  Hz, 2F, (pyridyl) $_2$ (naphth)C-F).

**Synthesis of  $[\text{Cu}_2(\mu\text{-}\eta^1\text{-}\eta^1\text{-OC}_6\text{F}_5)\text{DPFN}]\text{NTf}_2$  (**5**).** To a solution of  $[\text{Cu}_2(\mu\text{-}\eta^1\text{-}\eta^1\text{-Ph})\text{DPFN}]\text{NTf}_2$  (0.020 g, 0.020 mmol) in *o*-difluorobenzene (1.5 mL) was added a solution of pentafluorophenol (0.038 g, 0.21 mmol, 10 equiv) in *o*-difluorobenzene (1.0 mL) dropwise. The reaction mixture changed from dark green to dark orange and was stirred for 1.25 h. The mixture was then concentrated in vacuo, and the resulting residue was triturated with 3/2 pentane-toluene

(2.5 mL total) for 1.25 h. The resulting solid was allowed to settle, and the supernatant was carefully decanted. The dark solid was rinsed with pentane (3 × 1 mL) and then dissolved in THF (1.25 mL). This THF solution was filtered, and the filtrate was collected and cooled to −30 °C. Pentane (approximately 19 mL) was carefully layered on top of the cold filtrate, and storage for 1 day at −35 °C afforded a dark brown-gray solid. The supernatant was carefully decanted, and the solid was rinsed with pentane (3 × 1 mL). Residual volatile compounds were removed in vacuo to yield **5** as a dark solid (0.019 g, 0.017 mmol, 85%). Vapor diffusion of pentane into an *o*-difluorobenzene solution of **5** for 15 d at −35 °C afforded X-ray-quality crystals of 5-2-*o*-C<sub>6</sub>H<sub>4</sub>F<sub>2</sub>·0.5C<sub>5</sub>H<sub>12</sub>. <sup>1</sup>H NMR (600.13 MHz, THF-*d*<sub>6</sub>): δ 8.90 (d, *J* = 8.6 Hz, 2H, 4-naphth-C-H), 8.83 (dt, *J* = 5.0, 0.8 Hz, 4H, 6-pyridyl-C-H), 8.47 (dd, *J* = 8.6, 3.3 Hz, 2H, 3-naphth-C-H), 8.19 (dd, *J* = 8.2, 3.4 Hz, 4H, 3-pyridyl-C-H), 8.06 (td, *J* = 7.9, 1.8 Hz, 4H, 4-pyridyl-C-H), 7.56 (ddd, *J* = 7.7, 5.0, 1.2 Hz, 4H, 5-pyridyl-C-H). <sup>13</sup>C{<sup>1</sup>H} NMR (150.92 MHz, THF-*d*<sub>6</sub>): δ 160.36 (d, *J* = 30.1 Hz, 2-naphth-C), 154.17 (d, *J* = 30.1 Hz, 2-pyridyl-C), 150.62 (8a-naphth-C), 149.78 (d, *J* = 2.9 Hz, 6-pyridyl-C-H), 141.81 (d, *J* = 3.4 Hz, 4-naphth-C-H), 139.75 (d, *J* = 3.4 Hz, 4-pyridyl-C-H), 125.56 (5-pyridyl-C-H), 124.24 (4a-naphth-C), 121.44 (d, *J* = 14.8 Hz, 3-pyridyl-C-H), 121.03 (d, <sup>101</sup>*J* = 322.2 Hz, −SO<sub>2</sub>−CF<sub>3</sub>), 120.55 (d, *J* = 16.8 Hz, 3-naphth-C-H), 93.31 (d, *J* = 187.0 Hz, (pyridyl)<sub>2</sub>(naphth)C-F). Carbon resonances assignable to the pentafluorophenolate moiety were not observed. <sup>19</sup>F NMR (564.61 MHz, THF-*d*<sub>6</sub>): δ −79.08 (s, 6F, −SO<sub>2</sub>−CF<sub>3</sub>), −167.39 (dd, *J* = 20.0, 9.5 Hz, 2F, *ortho*-OC<sub>6</sub>F<sub>5</sub>), −168.31 (t, *J* = 21.5 Hz, 2F, *meta*-OC<sub>6</sub>F<sub>5</sub>), −170.88 (q, <sup>107</sup>*J* = 3.3 Hz, 2F, (pyridyl)<sub>2</sub>(naphth)C-F), −181.02 (tt, *J* = 22.3, 9.5 Hz, 1F, *para*-OC<sub>6</sub>F<sub>5</sub>). <sup>1</sup>H NMR (600.13 MHz, THF-*H*<sub>8</sub>): δ 8.90 (d, *J* = 8.6 Hz, 2H), 8.82 (d, *J* = 5.0 Hz, 4H), 8.46 (dd, *J* = 8.6, 3.3 Hz, 2H), 8.18 (dd, *J* = 8.3, 3.4 Hz, 4H), 8.06 (t, *J* = 7.9 Hz, 4H), 7.55 (dd, *J* = 7.6, 5.1 Hz, 4H). <sup>19</sup>F NMR (564.61 MHz, THF-*H*<sub>8</sub>): δ −79.04 (s, 6F), −167.35 (dd, *J* = 20.4, 9.5 Hz, 2F), −168.20 (t, *J* = 21.6 Hz, 2F), −170.89 (q, *J* = 3.8 Hz, 2F), −180.89 (tt, *J* = 22.8, 9.1 Hz, 1F). <sup>1</sup>H NMR (600.13 MHz, *o*-C<sub>6</sub>H<sub>4</sub>F<sub>2</sub>): δ 8.91 (d, *J* = 5.1 Hz, 4H), 8.37 (d, *J* = 8.6 Hz, 2H), 8.22 (dd, *J* = 8.6, 3.0 Hz, 2H), 8.00 (dd, *J* = 8.2, 3.4 Hz, 4H), 7.77 (td, *J* = 7.9, 1.7 Hz, 4H), 7.28 (dd, *J* = 7.6, 5.1 Hz, 4H). <sup>19</sup>F NMR (564.61 MHz, *o*-C<sub>6</sub>H<sub>4</sub>F<sub>2</sub>): δ −78.56 (s, 6F), −167.66 (t, *J* = 21.5 Hz, 2F), −167.89 (dd, *J* = 19.6, 8.7 Hz, 2F), −171.72 (d, *J* = 3.8 Hz, 2F), −179.74 (m, 1F). IR (ATR,  $\tilde{\nu}$  (cm<sup>−1</sup>)): 3116 (vw, br), 3093 (vw, br), 2961 (vw, br), 1647 (vw), 1605 (m), 1593 (m), 1575 (m), 1553 (vw), 1503 (s), 1472 (m), 1463 (m, sh), 1439 (m), 1429 (m, sh), 1351 (s), 1341 (s, sh), 1328 (m), 1302 (w), 1295 (w), 1260 (w), 1240 (w, sh), 1227 (m), 1202 (s, sh), 1179 (vs), 1160 (m, sh), 1133 (vs), 1103 (m), 1085 (m), 1058 (s), 1010 (s), 983 (s), 941 (w), 928 (w), 900 (vw), 891 (vw), 853 (m), 804 (m), 784 (s, sh), 769 (s), 755 (m), 739 (m), 710 (w), 698 (m), 685 (m), 654 (m), 644 (m, sh), 617 (s), 598 (s), 570 (vs), 532 (m), 508 (s), 482 (m), 463 (m), 454 (m), 428 (m), 416 (m). UV-vis (THF)  $\lambda_{\text{max}}$  nm ( $\epsilon$ , M<sup>−1</sup> cm<sup>−1</sup>/10<sup>3</sup>): 253 (24.4), 279 (sh 16.9), 305 (13.5), 317 (12.8), 347 (sh 4.77), 391 (3.44), 521 (0.923). Anal. Calcd for C<sub>38</sub>H<sub>20</sub>Cu<sub>3</sub>F<sub>13</sub>N<sub>7</sub>O<sub>5</sub>S<sub>2</sub>: C, 41.77; H, 1.84; N, 8.97. Found: C, 42.11; H, 1.67; N, 8.80.

**Synthesis of [Cu<sub>3</sub>(DPFN)<sub>2</sub>](NTf<sub>2</sub>)<sub>3</sub> (**6**).** A solution of triflimidic acid (0.0057 g, 0.020 mmol, 1.0 equiv) in *o*-difluorobenzene (1 mL) was added to a rapidly stirred solution of [Cu<sub>2</sub>( $\mu$ - $\eta^1$ - $\eta^1$ -Ph)DPFN]NTf<sub>2</sub> (0.0200 g, 0.020 mmol) in *o*-difluorobenzene (2 mL). Upon addition of the acid, the dark green solution became bright orange. The mixture was stirred for 1 h and then concentrated in vacuo to an orange oil that was then triturated by stirring with diethyl ether (7 mL) for 5 h. The resulting orange solid was allowed to settle, and the supernatant was carefully decanted. The orange solid was washed with diethyl ether (3 × 2 mL), and then residual volatile compounds were removed in vacuo. The solid was then dissolved in *o*-difluorobenzene (3 mL) and filtered, and the filtrate was cooled to −30 °C. Diethyl ether (17 mL) was carefully layered on top of the cold *o*-difluorobenzene solution, and storage for 2 days at −35 °C afforded a yellow-orange solid. The supernatant was carefully decanted, and the solid was rinsed with diethyl ether (3 × 3 mL). Residual volatile compounds were removed in vacuo to yield **6** as a bright yellow-orange

solid (0.0118 g, 0.0058 mmol, 58%). Vapor diffusion of hexanes into a *o*-C<sub>6</sub>H<sub>4</sub>F<sub>2</sub> solution of **6** for 4 days at −35 °C afforded X-ray-quality crystals of 6-2-*o*-C<sub>6</sub>H<sub>4</sub>F<sub>2</sub>. <sup>1</sup>H NMR (700.13 MHz, C<sub>6</sub>D<sub>5</sub>NO<sub>2</sub>): δ 9.33 (d, *J* = 8.6 Hz, 4H, 4-naphth-C-H), 8.45–8.39 (m, 8H, a-6-pyridyl-C-H and a-3-pyridyl-C-H), 8.36–8.29 (m, 8H, a-4-pyridyl-C-H and 3-naphth-C-H), 8.28–8.24 (m, 4H, b-3-pyridyl-C-H), 8.22 (td, *J* = 7.7, 1.8 Hz, 4H, b-4-pyridyl-C-H), 7.70–7.67 (m, 4H, a-5-pyridyl-C-H), 6.66 (m, 4H, b-6-pyridyl-C-H), 6.63 (m, 4H, b-5-pyridyl-C-H). <sup>108</sup> <sup>13</sup>C{<sup>1</sup>H} NMR (150.92 MHz, C<sub>6</sub>D<sub>5</sub>NO<sub>2</sub>): δ 161.37 (d, *J* = 29.1 Hz, 2-naphth-C), 156.41 (d, *J* = 30.4 Hz, a-2-pyridyl-C), 153.31 (d, *J* = 27.9 Hz, b-2-pyridyl-C), 152.50 (8a-naphth-C), 150.90 (a-6-pyridyl-C-H), 148.65 (b-6-pyridyl-C-H), <sup>109</sup> 143.22 (4-naphth-C-H), 141.09 (a-4-pyridyl-C-H), 139.87 (b-4-pyridyl-C-H), 126.95 (a-5-pyridyl-C-H), 126.49 (d, *J* = 4.2 Hz, 3-naphth-C-H), 125.62 (b-5-pyridyl-C-H), 124.74 (d, *J* = 16.6 Hz, b-3-pyridyl-C-H), 124.41 (s, 4a-naphth-C), 122.12 (d, *J* = 14.3 Hz, a-3-pyridyl-C-H), 121.50 (q, *J* = 321.9 Hz, −SO<sub>2</sub>−CF<sub>3</sub>), 96.19 (d, *J* = 180.8 Hz, (pyridyl)<sub>2</sub>(naphth)C-F). <sup>19</sup>F NMR (564.62 MHz, C<sub>6</sub>D<sub>5</sub>NO<sub>2</sub>): δ −78.18 (s, 18F, −SO<sub>2</sub>−CF<sub>3</sub>), −148.47 (s, 4F, (pyridyl)<sub>2</sub>(naphth)C-F). <sup>1</sup>H NMR (400.13 MHz, THF-*H*<sub>8</sub>): δ 9.04 (d, *J* = 8.8 Hz, 4H), 8.19 (t, *J* = 8.0 Hz, 5H), 8.01 (d, *J* = 4.5 Hz, 8H), 7.50 (t, *J* = 6.4 Hz, 4H), 6.44–6.34 (m, 4H), 6.31 (d, *J* = 5.3 Hz, 4H). <sup>19</sup>F NMR (376.44 MHz, THF-*H*<sub>8</sub>): δ −78.81 (s, 18F, −SO<sub>2</sub>−CF<sub>3</sub>), −148.38 (s, 4F, (pyridyl)<sub>2</sub>(naphth)C-F). <sup>1</sup>H NMR (600.13 MHz, *o*-C<sub>6</sub>H<sub>4</sub>F<sub>2</sub>): δ 8.63 (d, *J* = 8.6 Hz, 4H), 7.86 (d, *J* = 8.3 Hz, 4H), 7.70 (d, *J* = 5.1 Hz, 4H), 7.65–7.59 (m, 12H), 7.58–7.49 (m, 4H), 6.99 (dd, *J* = 7.6, 5.3 Hz, 4H), <sup>110</sup> 6.04 (m, *J* = 4.7 Hz, 8H). <sup>19</sup>F NMR (564.61 MHz, *o*-C<sub>6</sub>H<sub>4</sub>F<sub>2</sub>): δ −78.68 (s, 18F, −SO<sub>2</sub>−CF<sub>3</sub>), −149.32 (s, 4F, (pyridyl)<sub>2</sub>(naphth)C-F). IR (ATR,  $\tilde{\nu}$  (cm<sup>−1</sup>)): 3111 (vw), 3080 (vw, br), 3025 (vw), 1596 (w), 1575 (vw), 1507 (w), 1465 (w), 1439 (w), 1382 (w), 1349 (s), 1331 (m), 1303 (w), 1269 (vw), 1226 (m), 1180 (vs), 1132 (s), 1102 (w), 1052 (s), 1020 (m), 1011 (m), 969 (m), 941 (w), 933 (w), 902 (w, br), 858 (m), 807 (w), 772 (m), 754 (m), 739 (m), 710 (w), 695 (w), 686 (w), 651 (w), 613 (s), 598 (s), 569 (s), 532 (w), 509 (s), 470 (w), 454 (w), 424 (w). UV-vis (*o*-C<sub>6</sub>H<sub>4</sub>F<sub>2</sub>)  $\lambda_{\text{max}}$  nm ( $\epsilon$ , M<sup>−1</sup> cm<sup>−1</sup>/10<sup>3</sup>): 306.5 (20.4), 361 (sh 6.01), 422 (sh 2.68). Anal. Calcd for C<sub>66</sub>H<sub>40</sub>Cu<sub>3</sub>F<sub>22</sub>N<sub>15</sub>O<sub>12</sub>S<sub>6</sub>: C, 38.93; H, 1.98; N, 10.32. Found: C, 39.13; H, 1.90; N, 10.08.

**Reaction of [Cu<sub>2</sub>( $\mu$ - $\eta^1$ - $\eta^1$ -CH<sub>3</sub>)DPFN]NTf<sub>2</sub> with Pentafluorobenzene.** In a nitrogen-filled glovebox, **1** (0.001 g) was dissolved in THF (0.5 mL) containing a small drop of 1,3,5-tris(trifluoromethyl)benzene. The solution was placed in a J. Young tube that was then sealed, and baseline <sup>1</sup>H and <sup>19</sup>F NMR spectra were recorded. Then in a nitrogen-filled glovebox, a few drops of pentafluorobenzene (220 equiv, determined by <sup>1</sup>H and <sup>19</sup>F NMR spectroscopy) were added to the tube. The tube was sealed, and the first <sup>1</sup>H and <sup>19</sup>F NMR spectra were recorded within 5 min of pentafluorobenzene addition. The tube was allowed to stand at room temperature, and spectra were recorded at various intervals. After no change was observed at room temperature, the tube was heated at 60 °C, and the reaction mixture was monitored by <sup>1</sup>H and <sup>19</sup>F NMR spectra recorded at appropriately spaced intervals (Figure S10). After 14 days at 60 °C, the reaction mixture was concentrated in vacuo, and the resulting oil was dissolved in *o*-C<sub>6</sub>H<sub>4</sub>F<sub>2</sub>. The <sup>19</sup>F NMR spectra of the product in *o*-C<sub>6</sub>H<sub>4</sub>F<sub>2</sub> were consistent with previously reported spectra of [Cu<sub>2</sub>( $\mu$ - $\eta^1$ - $\eta^1$ -C<sub>6</sub>F<sub>5</sub>)DPFN]NTf<sub>2</sub>.<sup>25</sup>

**Reaction of [Cu<sub>2</sub>( $\mu$ - $\eta^1$ - $\eta^1$ -CH<sub>3</sub>)DPFN]NTf<sub>2</sub> with Water.** In a nitrogen-filled glovebox, **1** (0.001 g) was dissolved in THF (0.5 mL) containing 1,3,5-tris(trifluoromethyl)benzene (4.3 mM). The solution was placed in a J. Young tube that was then sealed, and baseline <sup>1</sup>H and <sup>19</sup>F NMR spectra were recorded. Then, the reaction mixture was frozen with liquid nitrogen, and the headspace of the J. Young tube was briefly evacuated under dynamic vacuum. Deaerated water was transferred under static vacuum into the reaction mixture, which remained immersed in liquid nitrogen. The amount of water transferred was estimated by the change in mass of the sealed tube. The reaction mixture was carefully thawed, and the reaction was monitored by <sup>19</sup>F NMR spectra recorded over the course of 2 weeks (Figure S11).

**Reaction of [Cu<sub>2</sub>( $\mu$ - $\eta^1$ - $\eta^1$ -CH<sub>3</sub>)DPFN]NTf<sub>2</sub> with Pentafluorophenol.** In a nitrogen-filled glovebox, a solution of **1** in THF

(0.5 mL, 2.2 mM, 1.1  $\mu\text{mol}$ ) was used to dissolve 1,3,5-trimethoxybenzene (0.0005 g, 3  $\mu\text{mol}$ ). The solution was placed in a J. Young tube that was then sealed, and baseline  $^1\text{H}$  and  $^{19}\text{F}$  NMR spectra were recorded. Then in a nitrogen-filled glovebox, pentafluorophenol (0.0020 g, 11  $\mu\text{mol}$ , 10 equiv) was added to the solution. The J. Young tube was sealed, and the reaction mixture began to change from green to yellow. The reaction was monitored by  $^1\text{H}$  and  $^{19}\text{F}$  NMR spectra recorded over the course of 1 h (Figures S12 and S13). The  $^1\text{H}$  and  $^{19}\text{F}$  product resonances of the product observed were consistent with those reported for  $[\text{Cu}_2(\mu\text{-}\eta^1\text{-OC}_6\text{F}_5)\text{DPFN}]\text{NTf}_2$  (vide supra).

**Reaction of  $[\text{Cu}_2(\mu\text{-}\eta^1\text{-CH}_3)\text{DPFN}]\text{NTf}_2$  with Triflimidic Acid.** In a nitrogen-filled glovebox, **1** (0.0023 g, 2.5  $\mu\text{mol}$ ) and 1,3,5-tris(trifluoromethyl)benzene (0.0042 g, 15  $\mu\text{mol}$ ) were dissolved in THF (0.5 mL). The solution was placed in a J. Young tube that was then sealed, and baseline  $^1\text{H}$  and  $^{19}\text{F}$  spectra were recorded. Then in a nitrogen-filled glovebox, in the tube was placed a solution of triflimidic acid (0.1 mL, 0.025 M, 2.5  $\mu\text{mol}$ , 1.0 equiv). The J. Young tube was sealed, and the reaction mixture began to change from green to orange.  $^1\text{H}$  and  $^{19}\text{F}$  NMR spectra were acquired 10 min after addition (Figure S14). The resonances observed for the mixture were consistent with those reported for  $[\text{Cu}_3(\text{DPFN})_2](\text{NTf}_2)_3$  (vide supra).

**Reaction of  $[\text{Cu}_2(\mu\text{-}\eta^1\text{-CH}_3)\text{DPFN}]\text{NTf}_2$  with Triphenylborane.** In a nitrogen-filled glovebox, a solution of **1** (0.55 mL, 2.0 mM, 1.1  $\mu\text{mol}$ ) in *o*-C<sub>6</sub>H<sub>4</sub>F<sub>2</sub> containing 1,3,5-tris(trifluoromethyl)benzene (2.6 mM) was prepared and placed in a J. Young tube that was then sealed. Baseline  $^1\text{H}$  and  $^{19}\text{F}$  NMR spectra were recorded. Then in a nitrogen-filled glovebox, to the solution was added triphenylborane (0.0026 g, 11  $\mu\text{mol}$ , 10 equiv). The triphenylborane dissolved, and the reaction mixture remained green. The J. Young tube was sealed, and the reaction was monitored by  $^1\text{H}$  and  $^{19}\text{F}$  NMR spectra recorded over the course of ca. 4 h (Figures S15 and S16). The  $^1\text{H}$  and  $^{19}\text{F}$  product resonances of the product observed were consistent with those reported for  $[\text{Cu}_2(\mu\text{-}\eta^1\text{-Ph})\text{DPFN}]\text{NTf}_2$  (see the Supporting Information). The appearance of a new downfield resonance at approximately 72.9 ppm (just beyond the resonance for BPh<sub>3</sub> at 67.3 ppm) in the  $^{11}\text{B}\{^1\text{H}\}$  NMR spectrum suggests the formation of BMePh<sub>2</sub> (Figure S17).<sup>75,76</sup>

**General Procedure for Exploring Reactivity between  $[\text{Cu}_2(\mu\text{-}\eta^1\text{-CH}_3)\text{DPFN}]\text{NTf}_2$  and Additional Liquid Reagents.** In a nitrogen-filled glovebox, a solution of **1** and an appropriate standard (1,3,5-tris(trifluoromethyl)benzene and/or 1,3,5-trimethoxybenzene) in THF was prepared and placed in a J. Young tube that was then sealed. Baseline  $^1\text{H}$  and  $^{19}\text{F}$  NMR spectra were recorded. Then, back in a nitrogen-filled glovebox, a given reagent was then added to the solution in the tube. The tube was resealed, and  $^1\text{H}$  and  $^{19}\text{F}$  NMR spectra were acquired. The reaction mixture was allowed to stand at room temperature (ca. 22 °C), and the reaction was monitored by  $^1\text{H}$  and  $^{19}\text{F}$  NMR spectra recorded at appropriate intervals. After no significant reaction was observed, the mixture was then heated to 60 or 80 °C, as specified in the main text, with  $^1\text{H}$  and  $^{19}\text{F}$  NMR spectra being acquired at appropriate intervals. In these reactions, heating led to decomposition, as suggested by the formation of methane and/or various fluorine-containing species.

**Procedure for Exploring Reactivity between  $[\text{Cu}_2(\mu\text{-}\eta^1\text{-CH}_3)\text{DPFN}]\text{NTf}_2$  and Carbon Dioxide.** In a nitrogen-filled glovebox, a solution of **1** (0.35 mL, 4.6 mM, 1.6  $\mu\text{mol}$ ) in THF-*d*<sub>8</sub> was prepared and placed in a J. Young tube that was then sealed. Baseline  $^1\text{H}$  NMR spectra were recorded. The tube was then cycled onto a Schlenk line, and the reaction mixture was degassed via three freeze–pump–thaw cycles. Carbon dioxide was then placed in the tube.  $^1\text{H}$  NMR spectra were recorded at appropriately spaced intervals while the reaction mixture was allowed to stand at room temperature (ca. 22 °C).  $^{13}\text{C}\{^1\text{H}\}$  NMR spectroscopy confirmed the addition of carbon dioxide. No reaction was observed after 29 h. The mixture was then heated to 60 °C for 2 days, during which only slight decomposition was observed, as indicated by the appearance of resonances assignable to methane and methane-*d*<sub>1</sub> in  $^1\text{H}$  NMR spectra of the mixture.

## ■ ASSOCIATED CONTENT

### 📄 Supporting Information

The Supporting Information is available free of charge on the ACS Publications website at DOI: 10.1021/acs.organomet.8b00443.

Cartesian coordinates of calculated structures of the cations of **1**, **2**, and **5**, as well as  $[\text{Cu}_2(\mu\text{-}\eta^1\text{-Ph})\text{DPFN}]^+$  and  $[\text{Cu}_2(\mu\text{-}\eta^1\text{-}\eta^1\text{-C}\equiv\text{C}(\text{C}_6\text{H}_5))\text{DPFN}]^+$  (XYZ)

Additional experimental details, supplementary figures and tables as described in the text, crystallographic figures and data, and computational figures and data (PDF)

### Accession Codes

CCDC 1578774–1578778 and 1840857 contain the supplementary crystallographic data for this paper. These data can be obtained free of charge via [www.ccdc.cam.ac.uk/data\\_request/cif](http://www.ccdc.cam.ac.uk/data_request/cif), or by emailing [data\\_request@ccdc.cam.ac.uk](mailto:data_request@ccdc.cam.ac.uk), or by contacting The Cambridge Crystallographic Data Centre, 12 Union Road, Cambridge CB2 1EZ, UK; fax: +44 1223 336033.

## ■ AUTHOR INFORMATION

### Corresponding Author

\*E-mail for T.D.T.: [tdtilley@berkeley.edu](mailto:tdtilley@berkeley.edu).

### ORCID

Micah S. Ziegler: 0000-0002-8549-506X

Daniel S. Levine: 0000-0001-8921-3659

T. Don Tilley: 0000-0002-6671-9099

### Present Address

<sup>§</sup>Institute for Data, Systems, and Society, Massachusetts Institute of Technology, Cambridge, Massachusetts 02139, United States.

### Notes

The authors declare no competing financial interest.

## ■ ACKNOWLEDGMENTS

This work was primarily funded by the U.S. Department of Energy, Office of Science, Office of Basic Energy Sciences, Chemical Sciences, Geosciences, and Biosciences Division, under Contract No. DE-AC02-05CH11231. We acknowledge the National Institutes of Health (NIH) for funding the UC Berkeley CheXray X-ray crystallographic facility under Grant No. S10-RR027172 and the UC Berkeley College of Chemistry NMR facility under Grant Nos. SRR023679A and 1S10RR016634-01. We also acknowledge Beamline 11.3.1 of Lawrence Berkeley National Laboratory's Advanced Light Source, which is a DOE Office of Science User Facility under Contract No. DE-AC02-05CH11231. In addition, M.S.Z. was supported by a National Science Foundation (NSF) Graduate Research Fellowship (Grant No. DGE 1106400) and a Philomathia Graduate Fellowship in the Environmental Sciences. We thank Prof. Richard A. Andersen and Dr. Eva M. Nichols for useful conversations. In addition, we thank Dr. Michael L. Aubrey for electrochemical equipment. Finally, we thank Dr. Antonio G. DiPasquale for X-ray crystallography advice and Dr. Jeffrey G. Pelton for NMR spectroscopy advice.

## ■ REFERENCES

- (1) Davidson, P. J.; Lappert, M. F.; Pearce, R. Stable Homoleptic Metal Alkyls. *Acc. Chem. Res.* 1974, 7 (7), 209–217.
- (2) Werner, H. Metal Alkyls and Metal Aryls: The “True” Transition Organometallics. In *Landmarks in Organo-Transition Metal Chem-*

istry. *Profiles in Inorganic Chemistry*; Springer: New York, 2009; pp 1–39.

(3) Braunstein, P.; Boag, N. M. Alkyl, Silyl, and Phosphane Ligands—Classical Ligands in Nonclassical Bonding Modes. *Angew. Chem., Int. Ed.* **2001**, *40* (13), 2427–2433.

(4) Campos, J.; López-Serrano, J.; Peloso, R.; Carmona, E. Methyl Complexes of the Transition Metals. *Chem. - Eur. J.* **2016**, *22* (19), 6432–6457.

(5) van Koten, G.; Perez, P.; Liebeskind, L. Introduction to the Ennobling a Base Metal: Presenting Copper in Organometallic Chemistry Issue. *Organometallics* **2012**, *31* (22), 7631–7633.

(6) Lipshutz, B. H. Organocopper Chemistry. In *Organometallics in Synthesis: A Manual*; Schlosser, M., Ed.; Wiley: New York, 2001; pp 665–815.

(7) Haseltine, J. N. Methylcopper. In *Encyclopedia of Reagents for Organic Synthesis*; Wiley: New York, 2001.

(8) Lipshutz, B. H.; Sengupta, S. Organocopper Reagents: Substitution, Conjugate Addition, Carbo/Metallocupration, and Other Reactions. In *Organic Reactions*; Wiley: New York, 2004.

(9) Posner, G. H. Conjugate Addition Reactions of Organocopper Reagents. In *Organic Reactions*; Wiley: New York, 2004.

(10) Yoshikai, N.; Nakamura, E. Mechanisms of Nucleophilic Organocopper(I) Reactions. *Chem. Rev.* **2012**, *112* (4), 2339–2372.

(11) Woodward, S. The Primary Organometallic in Copper-Catalyzed Reactions. In *Copper-Catalyzed Asymmetric Synthesis*; Alexakis, A., Krause, N., Woodward, S., Eds.; Wiley-VCH, 2014; pp 3–32.

(12) van Koten, G.; Jastrzebski, J. T. B. H. Structural Organocopper Chemistry. In *Chemistry of Functional Groups*; Patai, S., Ed.; Wiley: New York, 2009.

(13) Reich, M. R. Nouveaux composés organométalliques: le cuivre phényle et l'argent phényle. *Comptes Rendus Hebd. Séances Académie Sci.* **1923**, *177* (1), 322–326.

(14) Gilman, H.; Straley, J. M. Relative Reactivities of Organometallic Compounds. XIII. Copper and Silver. *Recl. Trav. Chim. Pays-Bas* **1936**, *55* (10), 821–834.

(15) Gilman, H.; Jones, R. G.; Woods, L. A. The Preparation of Methylcopper and Some Observations on the Decomposition of Organocopper Compounds. *J. Org. Chem.* **1952**, *17* (12), 1630–1634.

(16) Miyashita, A.; Yamamoto, T.; Yamamoto, A. Thermal Stability of Alkylcopper(I) Complexes Coordinated with Tertiary Phosphines. *Bull. Chem. Soc. Jpn.* **1977**, *50* (5), 1109–1117.

(17) Mankad, N. P.; Gray, T. G.; Laitar, D. S.; Sadighi, J. P. Synthesis, Structure, and CO<sub>2</sub> Reactivity of a Two-Coordinate (Carbene)Copper(I) Methyl Complex. *Organometallics* **2004**, *23* (6), 1191–1193.

(18) Goj, L. A.; Blue, E. D.; Delp, S. A.; Gunnoe, T. B.; Cundari, T. R.; Pierpont, A. W.; Petersen, J. L.; Boyle, P. D. Chemistry Surrounding Monomeric Copper(I) Methyl, Phenyl, Anilido, Ethoxide, and Phenoxide Complexes Supported by N-Heterocyclic Carbene Ligands: Reactivity Consistent with Both Early and Late Transition Metal Systems. *Inorg. Chem.* **2006**, *45* (22), 9032–9045.

(19) Thiele, K.-H.; Köhler, J. Zur Darstellung von Alkyl-Kupfer-Verbindungen. *J. Organomet. Chem.* **1968**, *12* (1), 225–229.

(20) Ikariya, T.; Yamamoto, A. Preparation and Properties of Ligand-Free Methylcopper and of Copper Alkyls Coordinated with 2,2'-Bipyridyl and Tricyclohexylphosphine. *J. Organomet. Chem.* **1974**, *72* (1), 145–151.

(21) Villacorta, G. M.; Rao, C. P.; Lippard, S. J. Synthesis and Reactivity of Binuclear Tropocoronand and Related Organocopper(I) Complexes. Catalytic Enantioselective Conjugate Addition of Grignard Reagents to 2-Cyclohexen-1-One. *J. Am. Chem. Soc.* **1988**, *110* (10), 3175–3182.

(22) Dempsey, D. F.; Girolami, G. S. Copper(I) Alkyls. Synthesis and Characterization of Tertiary Phosphine Adducts and the Crystal Structure of the Dimethylcuprate Complex [Cu(PMe<sub>3</sub>)<sub>4</sub>][CuMe<sub>2</sub>]. *Organometallics* **1988**, *7* (5), 1208–1213.

(23) Hope, H.; Olmstead, M. M.; Power, P. P.; Sandell, J.; Xu, X. Isolation and X-Ray Crystal Structures of the Mononuclear Cuprates

[CuMe<sub>2</sub>]<sup>-</sup>, [CuPh<sub>2</sub>]<sup>-</sup>, and [Cu(Br)CH(SiMe<sub>3</sub>)<sub>2</sub>]<sup>-</sup>. *J. Am. Chem. Soc.* **1985**, *107* (14), 4337–4338.

(24) John, M.; Auel, C.; Behrens, C.; Marsch, M.; Harms, K.; Bosold, F.; Gschwind, R. M.; Rajamohanam, P. R.; Boche, G. The Relation between Ion Pair Structures and Reactivities of Lithium Cuprates. *Chem. - Eur. J.* **2000**, *6* (16), 3060–3068.

(25) Ziegler, M. S.; Levine, D. S.; Lakshmi, K. V.; Tilley, T. D. Aryl Group Transfer from Tetraarylboration Anions to an Electrophilic Dicopper(I) Center and Mixed-Valence  $\mu$ -Aryl Dicopper(I,II) Complexes. *J. Am. Chem. Soc.* **2016**, *138* (20), 6484–6491.

(26) Ziegler, M. S.; Lakshmi, K. V.; Tilley, T. D. Dicopper Cu(I)Cu(I) and Cu(I)Cu(II) Complexes in Copper-Catalyzed Azide–Alkyne Cycloaddition. *J. Am. Chem. Soc.* **2017**, *139* (15), 5378–5386.

(27) Lusch, M. J.; Phillips, W. V.; Sieloff, R. F.; Nomura, G. S.; House, H. O.; Bisacchi, G. S.; Stevens, R. V. Preparation of Low-Halide Methylolithium. *Org. Synth.* **1984**, *62*, 101.

(28) Rathman, T. L.; Araki, S.; Hirashita, T. Methylolithium. In *Encyclopedia of Reagents for Organic Synthesis*; Wiley: New York, 2001.

(29) Molteni, R.; Bertermann, R.; Edkins, K.; Steffen, A. An Unexpected Transmetalation Intermediate: Isolation and Structural Characterization of a Solely CH<sub>3</sub> Bridged Di-Copper(I) Complex. *Chem. Commun.* **2016**, *52* (28), 5019–5022.

(30) Ma, G.; Ferguson, M. J.; McDonald, R.; Cavell, R. G. Rare, Hexatomic, Boat-Shaped, Cross-Linked Bis-(Iminodiphenylphosphorano)Methanediide Pincer Carbon Bridged Photoluminescent Copper Clusters Capped with Methyl or Halide Bridges. *Organometallics* **2010**, *29* (19), 4251–4264.

(31) Tate, B. K.; Jordan, A. J.; Bacsá, J.; Sadighi, J. P. Stable Mono- and Dinuclear Organosilver Complexes. *Organometallics* **2017**, *36* (5), 964–974.

(32) Espada, M. F.; Campos, J.; López-Serrano, J.; Poveda, M. L.; Carmona, E. Methyl-, Ethenyl-, and Ethynyl-Bridged Cationic Digold Complexes Stabilized by Coordination to a Bulky Terphenylphosphine Ligand. *Angew. Chem., Int. Ed.* **2015**, *54* (51), 15379–15384.

(33) Vranka, R. G.; Amma, E. L. Crystal Structure of Trimethylaluminum. *J. Am. Chem. Soc.* **1967**, *89* (13), 3121–3126.

(34) Tugarinov, V.; Hwang, P. M.; Ollerenshaw, J. E.; Kay, L. E. Cross-Correlated Relaxation Enhanced <sup>1</sup>H–<sup>13</sup>C NMR Spectroscopy of Methyl Groups in Very High Molecular Weight Proteins and Protein Complexes. *J. Am. Chem. Soc.* **2003**, *125* (34), 10420–10428.

(35) Tritto, I.; Sacchi, M. C.; Locatelli, P.; Li, S. X. Low-Temperature <sup>1</sup>H and <sup>13</sup>C NMR Investigation of Trimethylaluminum Contained in Methylaluminumoxane Cocatalyst for Metallocene-Based Catalysts in Olefin Polymerization. *Macromol. Chem. Phys.* **1996**, *197* (4), 1537–1544.

(36) Gärtner, T.; Gschwind, R. M. NMR of Organocopper Compounds. In *PATAI'S Chemistry of Functional Groups*; Wiley: New York, 2009.

(37) Pasykiewicz, S.; Popławska, J. Thermal Decomposition of Methylcopper and Methyl(Tricyclohexylphosphine)Copper. *J. Organomet. Chem.* **1985**, *282* (3), 427–434.

(38) Muller, N.; Pritchard, D. E. C<sup>13</sup> Splittings in Proton Magnetic Resonance Spectra. I. Hydrocarbons. *J. Chem. Phys.* **1959**, *31* (3), 768–771.

(39) Yamamoto, O. <sup>27</sup>Al–<sup>13</sup>C Coupling Constants in Trimethylaluminum Dimer and Its Derivatives. *J. Chem. Phys.* **1975**, *63* (7), 2988–2995.

(40) House, H. O.; Respass, W. L.; Whitesides, G. M. The Chemistry of Carbanions. XII. The Role of Copper in the Conjugate Addition of Organometallic Reagents. *J. Org. Chem.* **1966**, *31* (10), 3128–3141.

(41) Maslowsky, E. Alkyl Organometallic Derivatives. In *Vibrational Spectra of Organometallic Compounds*; Wiley: New York, 1977; p 564.

(42) Chai, J.-D.; Head-Gordon, M. Long-Range Corrected Hybrid Density Functionals with Damped Atom–Atom Dispersion Corrections. *Phys. Chem. Chem. Phys.* **2008**, *10* (44), 6615–6620.

- (43) Yamamoto, A.; Miyashita, A.; Yamamoto, T.; Ikeda, S. Preparation and Properties of Methylcopper-Triphenylphosphine Complexes. *Bull. Chem. Soc. Jpn.* **1972**, *45* (5), 1583–1583.
- (44) Costa, G.; Alti, G. D.; Stefani, L.; Bosca-Rato, G. Sulla Decomposizione Termica Del Rame-Metile. *Ann. Chim.* **1962**, *52*, 289–304.
- (45) Miyashita, A.; Yamamoto, A. Preparation and Properties of Stable Alkylcopper(I) Complexes Containing Tertiary Phosphine Ligands. *Bull. Chem. Soc. Jpn.* **1977**, *50* (5), 1102–1108.
- (46) Goj, L. A.; Blue, E. D.; Munro-Leighton, C.; Gunnoe, T. B.; Petersen, J. L. Cleavage of X–H Bonds (X = N, O, or C) by Copper(I) Alkyl Complexes To Form Monomeric Two-Coordinate Copper(I) Systems. *Inorg. Chem.* **2005**, *44* (24), 8647–8649.
- (47) Andersen, R. A.; Carmona-Guzman, E.; Gibson, J. F.; Wilkinson, G. Neopentyl, Neophyl, and Trimethylsilylmethyl Compounds of Manganese. Manganese(II) Dialkyls; Manganese(II) Dialkyl Amine Adducts; Tetra-Alkylmanganate(II) Ions and Lithium Salts; Manganese(IV) Tetra-Alkyls. *J. Chem. Soc., Dalton Trans. J. Chem. Soc., Dalton Trans.* **1976**, *21*, 2204–2211.
- (48) Howard, C. G.; Wilkinson, G.; Thornton-Pett, M.; Hursthouse, M. B. Tertiary Phosphine Adducts of Manganese(II) Dialkyls. Part I. Synthesis, Properties and Structures of Alkyl-Bridged Dimers. *J. Chem. Soc., Dalton Trans.* **1983**, *9*, 2025–2030.
- (49) Koschmieder, S. U.; Wilkinson, G.; Hussain-Bates, B.; Hursthouse, M. B. Reactions of Organic Isocyanates and Tert-Butyl Isocyanide with Manganese(II) Alkyls and Trimesitylchromium. *J. Chem. Soc., Dalton Trans.* **1992**, *1*, 19–24.
- (50) Price, J. S.; Chadha, P.; Emslie, D. J. H. Base-Free and Bisphosphine Ligand Dialkylmanganese(II) Complexes as Precursors for Manganese Metal Deposition. *Organometallics* **2016**, *35* (2), 168–180.
- (51) Hartner, F. W.; Schwartz, J. Synthesis and Characterization of “Long-Chain” Alkylidene-Bridged Hetero Bimetallic Complexes. *J. Am. Chem. Soc.* **1981**, *103* (16), 4979–4981.
- (52) Hao, S.; Song, J.-I.; Berno, P.; Gambarotta, S. Chromium(II) Organochromates. Preparation, Characterization, and Stability. *Organometallics* **1994**, *13* (4), 1326–1335.
- (53) Jarvis, J. A. J.; Pearce, R.; Lappert, M. F. Silylmethyl and Related Complexes. Part 4. Preparation, Properties, and Crystal and Molecular Structure of Tetrakis[(Trimethylsilylmethyl)-Copper(I)], an Alkyl-Bridged, Square-Planar, Tetranuclear Copper(I) Cluster. *J. Chem. Soc., Dalton Trans.* **1977**, *10*, 999–1003.
- (54) Kochi, J. K.; Wada, K.; Tamura, M. Autocatalytic Decomposition of Alkylcopper(I) Species. Electron Spin Resonance Spectrum of Binuclear Copper(0) Intermediates. *J. Am. Chem. Soc.* **1970**, *92* (22), 6656–6658.
- (55) Tamura, M.; Kochi, J. K. The Reactions of Grignard Reagents with Transition Metal Halides: Coupling, Disproportionation, and Exchange with Olefins. *Bull. Chem. Soc. Jpn.* **1971**, *44* (11), 3063–3073.
- (56) Tamura, M.; Kochi, J. K. Copper-Catalyzed Coupling of Grignard Reagents and Alkyl Halides in Tetrahydrofuran Solutions. *J. Organomet. Chem.* **1972**, *42* (1), 205–228.
- (57) MacPhee, J. A.; Boussu, M.; Dubois, J.-E. Grignard Reagent–Acid Chloride Condensation in the Presence of Copper(I) Chloride. A Study of Structural Effects by Direct and Competition Methods. *J. Chem. Soc., Perkin Trans. 2* **1974**, *12*, 1525–1530.
- (58) Commercon, A.; Normant, J.; Villieras, J. Substitution of Vinylic Iodides by Various Copper(I) and Copper(II) Derivatives. *J. Organomet. Chem.* **1975**, *93* (3), 415–421.
- (59) Lutz, C.; Jones, P.; Knochel, P. Neopentyl and Neophyl Groups: New Nontransferable Groups for Organocopper and Organozinc Chemistry. *Synthesis* **1999**, *1999* (02), 312–316.
- (60) Fraenkel, G.; Chow, A.; Winchester, W. R. Structure and Dynamic Behavior of Solvated Neopentyllithium Monomers, Dimers, and Tetramers: Proton, Carbon-13 and Lithium-6 NMR. *J. Am. Chem. Soc.* **1990**, *112* (17), 6190–6198.
- (61) Davidson, P. J.; Lappert, M. F.; Pearce, R. Metal  $\sigma$ -Hydrocarbyls, MR<sub>n</sub>. Stoichiometry, Structures, Stabilities, and Thermal Decomposition Pathways. *Chem. Rev.* **1976**, *76* (2), 219–242.
- (62) Crabtree, R. H. Alkyls and Hydrides. In *The Organometallic Chemistry of the Transition Metals*; Wiley: Hoboken, NJ, 2014; pp 69–97.
- (63) Muller, N.; Pritchard, D. E. C<sup>13</sup> Splittings in Proton Magnetic Resonance Spectra. II. Bonding in Substituted Methanes. *J. Chem. Phys.* **1959**, *31* (6), 1471–1476.
- (64) Pople, J. A.; McIver, J. W.; Ostlund, N. S. Self-Consistent Perturbation Theory. II. Nuclear-Spin Coupling Constants. *J. Chem. Phys.* **1968**, *49* (7), 2965–2970.
- (65) Newton, M. D.; Schulman, J. M.; Manus, M. M. Theoretical Studies of Benzene and Its Valence Isomers. *J. Am. Chem. Soc.* **1974**, *96* (1), 17–23.
- (66) Bingel, W. A.; Lüttke, W. Hybrid Orbitals and Their Applications in Structural Chemistry. *Angew. Chem., Int. Ed. Engl.* **1981**, *20* (11), 899–911.
- (67) Waack, R.; Doran, M. A.; Baker, E. B.; Olah, G. A. Nuclear Magnetic Resonance Investigation of  $\alpha$ -C<sup>13</sup>-Phenylmethylolithiums. *J. Am. Chem. Soc.* **1966**, *88* (6), 1272–1275.
- (68) McKeever, L. D.; Waack, R.; Doran, M. A.; Baker, E. B. Nuclear Magnetic Resonance Study of Structure and Bonding in Methylithium. *J. Am. Chem. Soc.* **1969**, *91* (5), 1057–1061.
- (69) Reich, H. J. 6.5 One-Bond Carbon-Proton Coupling (<sup>1</sup>J<sub>CH</sub>); <https://www.chem.wisc.edu/areas/reich/nmr/06-cmr-05-1jch.htm> (accessed Dec 11, 2017).
- (70) King, A. E.; Brunold, T. C.; Stahl, S. S. Mechanistic Study of Copper-Catalyzed Aerobic Oxidative Coupling of Arylboronic Esters and Methanol: Insights into an Organometallic Oxidase Reaction. *J. Am. Chem. Soc.* **2009**, *131* (14), 5044–5045.
- (71) King, A. E.; Ryland, B. L.; Brunold, T. C.; Stahl, S. S. Kinetic and Spectroscopic Studies of Aerobic Copper(II)-Catalyzed Methoxylation of Arylboronic Esters and Insights into Aryl Transmetalation to Copper(II). *Organometallics* **2012**, *31* (22), 7948–7957.
- (72) Verma, A.; Santos, W. L. Copper-Catalyzed Coupling Reactions of Organoboron Compounds. In *Boron Reagents in Synthesis*; American Chemical Society, 2016; ACS Symposium Series Vol. 1236, pp 313–356.
- (73) Vantourout, J. C.; Miras, H. N.; Isidro-Llobet, A.; Sproules, S.; Watson, A. J. B. Spectroscopic Studies of the Chan–Lam Amination: A Mechanism-Inspired Solution to Boronic Ester Reactivity. *J. Am. Chem. Soc.* **2017**, *139* (13), 4769–4779.
- (74) Vasilopoulos, A.; Zultanski, S. L.; Stahl, S. S. Feedstocks to Pharmacophores: Cu-Catalyzed Oxidative Arylation of Inexpensive Alkylarenes Enabling Direct Access to Diarylalkanes. *J. Am. Chem. Soc.* **2017**, *139* (23), 7705–7708.
- (75) Wrackmeyer, B.; Nöth, H. Kernresonanzspektroskopische Untersuchungen an Bor-Verbindungen, X: <sup>11</sup>B-, <sup>14</sup>N- und <sup>1</sup>H-Kernresonanzuntersuchungen an Boryl-Substituiertem Thiophen, Furan, N-Methylpyrrol und Verwandten Systemen. Beurteilung der Wechselwirkung Zwischen sp<sup>2</sup>-Hybridisiertem Bor und  $\pi$ -Systemen. *Chem. Ber.* **1976**, *109* (3), 1075–1088.
- (76) *Nuclear Magnetic Resonance Spectroscopy of Boron Compounds*; Nöth, H., Wrackmeyer, B., Eds.; Springer Berlin Heidelberg: Berlin, Heidelberg, 1978.
- (77) Kundu, S.; Greene, C.; Williams, K. D.; Salvador, T. K.; Bertke, J. A.; Cundari, T. R.; Warren, T. H. Three-Coordinate Copper(II) Aryls: Key Intermediates in C–O Bond Formation. *J. Am. Chem. Soc.* **2017**, *139* (27), 9112–9115.
- (78) Miyashita, A.; Yamamoto, A. Insertion of Carbon Dioxide into the Cu–CH<sub>3</sub> Bond of Methylbis(Triphenylphosphine)Copper Etherate. *J. Organomet. Chem.* **1973**, *49* (1), C57–C58.
- (79) Miyasuta, A.; Yamamoto, A. Insertion Reactions of Carbon Dioxide and Carbon Disulfide into Alkyl-Copper Bonds of Alkylcopper(I) Complexes Having Tertiary Phosphine Ligands. *J. Organomet. Chem.* **1976**, *113* (2), 187–199.
- (80) Camus, A.; Marsich, N.; Nardin, G.; Randaccio, L. The Crystal Structure of *o*-Anisylcopper(I): An Octameric Copper(I) Cluster Compound. *J. Organomet. Chem.* **1979**, *174* (1), 121–128.

- (81) Zhang, S.; Fallah, H.; Gardner, E. J.; Kundu, S.; Bertke, J. A.; Cundari, T. R.; Warren, T. H. A Dinitrogen Dicopper(I) Complex via a Mixed-Valence Dicopper Hydride. *Angew. Chem., Int. Ed.* **2016**, *55* (34), 9927–9931.
- (82) Liu, S.; Eberhart, M. S.; Norton, J. R.; Yin, X.; Neary, M. C.; Paley, D. W. Cationic Copper Hydride Clusters Arising from Oxidation of  $(\text{Ph}_3\text{P})_6\text{Cu}_6\text{H}_6$ . *J. Am. Chem. Soc.* **2017**, *139* (23), 7685–7688.
- (83) Goj, L. A.; Blue, E. D.; Delp, S. A.; Gunnoe, T. B.; Cundari, T. R.; Petersen, J. L. Single-Electron Oxidation of Monomeric Copper(I) Alkyl Complexes: Evidence for Reductive Elimination through Bimolecular Formation of Alkanes. *Organometallics* **2006**, *25* (17), 4097–4104.
- (84) Davenport, T. C.; Tilley, T. D. Dinucleating Naphthyridine-Based Ligand for Assembly of Bridged Dicopper(I) Centers: Three-Center Two-Electron Bonding Involving an Acetonitrile Donor. *Angew. Chem., Int. Ed.* **2011**, *50* (51), 12205–12208.
- (85) Green, J. C.; Green, M. L. H.; Parkin, G. The Occurrence and Representation of Three-Centre Two-Electron Bonds in Covalent Inorganic Compounds. *Chem. Commun.* **2012**, *48* (94), 11481–11503.
- (86) Levine, D. S.; Horn, P. R.; Mao, Y.; Head-Gordon, M. Variational Energy Decomposition Analysis of Chemical Bonding. 1. Spin-Pure Analysis of Single Bonds. *J. Chem. Theory Comput.* **2016**, *12* (10), 4812–4820.
- (87) Levine, D. S.; Head-Gordon, M. Energy Decomposition Analysis of Single Bonds within Kohn–Sham Density Functional Theory. *Proc. Natl. Acad. Sci. U. S. A.* **2017**, *114* (48), 12649–12656.
- (88) Cope, A. C. The Preparation of Dialkylmagnesium Compounds from Grignard Reagents. *J. Am. Chem. Soc.* **1935**, *57* (11), 2238–2240.
- (89) Hoye, T. R.; Eklov, B. M.; Voloshin, M. No-D NMR Spectroscopy as a Convenient Method for Titering Organolithium (RLi), RMgX, and LDA Solutions. *Org. Lett.* **2004**, *6* (15), 2567–2570.
- (90) Schrock, R. R.; Fellmann, J. D. Multiple Metal–Carbon Bonds. 8. Preparation, Characterization, and Mechanism of Formation of the Tantalum and Niobium Neopentylidene Complexes,  $\text{M}(\text{CH}_2\text{CMe}_3)_3(\text{CHCMe}_3)$ . *J. Am. Chem. Soc.* **1978**, *100* (11), 3359–3370.
- (91) Schrock, R. R.; Sancho, J.; Pederson, S. F.; Virgil, S. C.; Grubbs, R. H. 2, 2-Dimethylpropylidyne Tungsten(VI) Complexes and Precursors for Their Syntheses. In *Inorganic Syntheses*; Kaesz, H. D., Ed.; Wiley: New York, 1989; pp 44–51.
- (92) Fulmer, G. R.; Miller, A. J. M.; Sherden, N. H.; Gottlieb, H. E.; Nudelman, A.; Stoltz, B. M.; Bercaw, J. E.; Goldberg, K. I. NMR Chemical Shifts of Trace Impurities: Common Laboratory Solvents, Organics, and Gases in Deuterated Solvents Relevant to the Organometallic Chemist. *Organometallics* **2010**, *29* (9), 2176–2179.
- (93) Harris, R. K.; Becker, E. D.; Cabral de Menezes, S. M.; Goodfellow, R.; Granger, P. NMR Nomenclature: Nuclear Spin Properties and Conventions for Chemical Shifts. IUPAC Recommendations 2001. International Union of Pure and Applied Chemistry. Physical Chemistry Division. Commission on Molecular Structure and Spectroscopy. *Magn. Reson. Chem.* **2002**, *40* (7), 489–505.
- (94) Sheldrick, G. M. A Short History of SHELX. *Acta Crystallogr., Sect. A: Found. Crystallogr.* **2008**, *64* (1), 112–122.
- (95) Sheldrick, G. M. SHELXT – Integrated Space-Group and Crystal-Structure Determination. *Acta Crystallogr., Sect. A: Found. Adv.* **2015**, *71* (1), 3–8.
- (96) Spek, A. L. PLATON SQUEEZE: A Tool for the Calculation of the Disordered Solvent Contribution to the Calculated Structure Factors. *Acta Crystallogr., Sect. C: Struct. Chem.* **2015**, *71* (1), 9–18.
- (97) Shao, Y.; Gan, Z.; Epifanovsky, E.; Gilbert, A. T. B.; Wormit, M.; Kussmann, J.; Lange, A. W.; Behn, A.; Deng, J.; Feng, X.; et al. Advances in Molecular Quantum Chemistry Contained in the Q-Chem 4 Program Package. *Mol. Phys.* **2015**, *113* (2), 184–215.
- (98) Gilbert, A. *IQmol*.
- (99) CCCBDB Vibrational frequency scaling factors; <https://cccbdb.nist.gov/vibnotes.asp> (accessed Mar 21, 2018).
- (100) CCCBDB listing of precalculated vibrational scaling factors; <https://cccbdb.nist.gov/vibscalejust.asp> (accessed Mar 21, 2018).
- (101) This doublet is presumably the central two resonances of a quartet assignable to the triflimide anion  $-\text{SO}_2-\text{CF}_3$ .
- (102) With very good shimming, this resonance appears as a slightly broadened quartet. However, spin simulation (of an  $\text{AX}_2\text{Y}$  system with  $J_{\text{AX}} = 3.36$  Hz and  $J_{\text{AY}} = 3.14$  Hz in THF- $d_8$ ) suggests that it is a triplet of doublets, as expected for the  $^{19}\text{F}$  resonance being split by two equivalent pyridyl protons (3-pyridyl-C–H) and one naphthyridine proton (3-naphth-C–H).
- (103) This resonance was observed on the downfield shoulder of the solvent ( $o\text{-C}_6\text{H}_4\text{F}_2$ ) resonance.
- (104) Spin simulation (of an  $\text{AX}_2\text{Y}$  system with  $J_{\text{AX}} = 3.37$  Hz, and  $J_{\text{AY}} = 3.22$  Hz in THF- $d_8$ ) suggests that this apparent quartet is a triplet of doublets, as described earlier.
- (105) Spin simulation (of an  $\text{AX}_2\text{Y}$  system with  $J_{\text{AX}} = 2.43$  Hz, and  $J_{\text{AY}} = 3.13$  Hz in THF- $d_8$ ) suggests that this apparent quartet is a triplet of doublets, as described earlier.
- (106) Spin simulation (of an  $\text{AX}_2\text{Y}$  system with  $J_{\text{AX}} = 3.24$  Hz, and  $J_{\text{AY}} = 3.15$  Hz in THF- $d_8$ ) suggests that this apparent quartet is a triplet of doublets, as described earlier.
- (107) Spin simulation (of an  $\text{AX}_2\text{Y}$  system with  $J_{\text{AX}} = 3.45$  Hz, and  $J_{\text{AY}} = 3.30$  Hz in THF- $d_8$ ) suggests that this apparent quartet is a triplet of doublets, as described earlier.
- (108) Loss of symmetry splits the “side-arm” pyridine moieties into two sets of two pyridines. They are separately labeled with a and b. This notation is conserved in the  $^{13}\text{C}\{^1\text{H}\}$  NMR assignments.
- (109) These proton and carbon resonances overlapped with or were obscured by solvent resonances, other complex resonances, or otherwise not observed directly and instead observed and assigned via  $^1\text{H}-^1\text{H}$  COSY and  $^1\text{H}-^{13}\text{C}$  HSQC and HMBC experiments.
- (110) These resonances were observed on the shoulders of the solvent ( $o\text{-C}_6\text{H}_4\text{F}_2$ ) resonance.